Cluster virial expansion for the equation of state of partially ionized hydrogen plasma

Dissertation
zur
Erlangung des akademischen Grades
doctor rerum naturalium (Dr. rer. nat.)
der Mathematisch-Naturwissenschaftlichen Fakultät
der Universität Rostock

vorgelegt von
Yultuz Omarbakiyeva, geb. am 19.11.1981
in Tigermen, Almaty Gebiet, Kasachstan
aus Rostock

Rostock, 30. November 2010

Liste der Gutachter

- Prof. Dr. Gerd Röpke
  Institut für Physik
  Universität Rostock

- Prof. Dr. Ronald Redmer
  Institut für Physik
  Universität Rostock

Datum der Verteidigung: 30. November 2010

für meine Eltern:
Omarbakiyev Amurullam
und
Maxatova Tamarakhan

Abstract

The electron-atom interaction in a partially-ionized hydrogen plasma is the topic of this work. The transport and the thermodynamical properties of dense hydrogen plasma is studied with relation to interaction between electrons and hydrogen atoms with including of environment effects. The properties of the often used effective potentials for electron-atom interaction are considered. Some kinetic characteristics such as phase shifts and cross sections are calculated on the basis of polarization pseudopotential models and separable models. The main part of this work is devoted to the contribution of electron-atom interaction to the equation of state for partially ionized hydrogen plasma, which is studied using the cluster-virial expansion. Within the Beth-Uhlenbeck approach, the second virial coefficient for the electron-atom (bound cluster) pair is related to the scattering phase-shifts and binding energies. Experimental phase-shifts as well as phase-shifts calculated on the basis of different pseudopotential models are used as an input for the Beth-Uhlenbeck formula. By including Pauli blocking and screening, the generalized second virial coefficient can be applied to a larger region in the temperature-density plane. We present results for the electron-atom contribution to the virial expansion and the corresponding equation of state, i.e. the pressure, composition, and chemical potentials as a function of density and temperature. These results are compared with semi-empirical approaches to the thermodynamics of partially ionized plasmas. Avoiding any ill-founded input quantities, the Beth-Uhlenbeck second virial coefficient for the electron-atom interaction, presented here for the first time, can be considered as a benchmark for other, semi-empirical approaches.

Contents

Part I

Cluster virial expansion for the equation of state of partially ionized hydrogen plasma

Chapter 1

Introduction

1.1 Plasmas

A plasma is an ionised gas, consisting of free electrons, ions and atoms or molecules, which is characterised by its collective behaviour. The charged particles in a plasma are coupled by electric and magnetic self-generated and self-consistent fields [Sch05].

Examples of plasma can be met on the Earth in the form of a lightning, flame and the ionosphere surrounding our planet. In fact many astrophysical objects consist of plasma as white dwarfs, giant planets, stars etc. In laboratories a nonideal plasmas are generated by heating of solid, liquid, or gasous targets so as to thermaly ionize a high fraction of electrons. This can also be achieved through compression of solid targets, using the so-called pressure induced ionization [FY98]. Currently, so-called non-ideal plasmas represent a rapidly evolving field of research. Non-ideal plasmas are characterized by the ratio of average interaction energy of two particles at their mean distance to their kinetic energy or temperature [FY98, WDWG86, KSK05].

From one side, non-ideal plasmas are observed in various astrophysical objects such as interiors of Jupiter and Saturn [RHJ$^+$06a, LHR09], or white dwarfs [Dra06]; shockwaves with compressions and heating of plasma up to several thousand degrees at pressures of several hundred thousand atmospheres [MF06].

Experimental and theoretical studies of non-ideal plasmas are among the most challenging tasks in today's science. This is mainly stipulated by the fact that plasma at high temperatures and pressures becomes thermally aggressive. Also, theoretical studies and numerical simulations establish challenging tasks requiring original approaches to solutions.

It is usefull to introduce the main plasma parameters and to make the classification of plasmas. The basic parameters of the plasma are temperature and number density. These parameters span the so-called plasma phase space, or n-T diagram, which allows for a systematic representation of various types of plasmas. An example is shown in Fig. 1.1, including astrophysical plasmas and realisations in the laboratory.

An important quantity for a plasma is the coupling or nonideality parameter, which
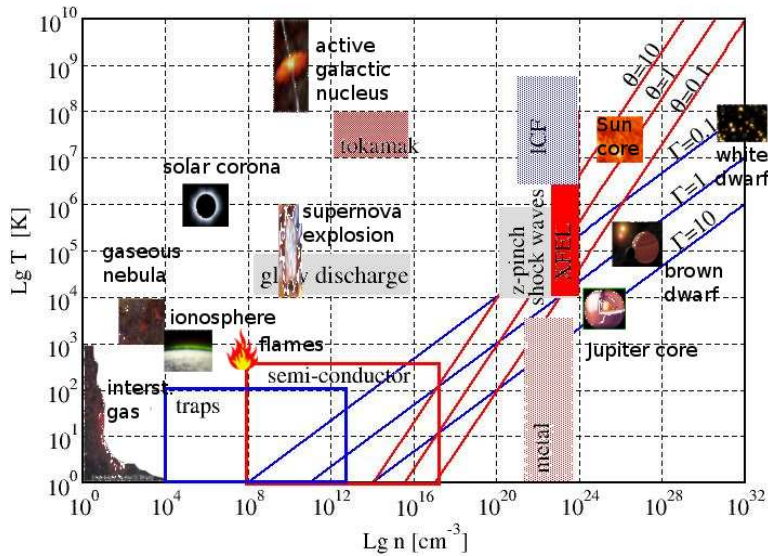
Figure 1.1: Examples of plasma in the density-temperature plane Ref. [Red05].

was already discussed above. It is defined as

$$\Gamma = \frac{e^2}{4\pi\epsilon_0 a k_B T} \ . \tag{1.1}$$

The coupling parameter quantifies relative importance of the particle's electrical interaction energy and thermal energy. Here k_B is the Boltzmann's constant, $a = (\frac{3}{4\pi n})^{1/3}$ is interparticle distance. n and T are the number density and the temperature, respectively, which can be different for each species as ions and electrons. Plasma is ideal or weakly coupled, if $\Gamma < 1$. This means that individual particles feel each other very weakly and can be considered as gaseous state. Strongly coupled or non-ideal plasmas corresponds to $\Gamma > 1$. In such systems, particles can not be considered as free particles and interaction between particles become important.

The plasma becomes degenarate, if plasma density is high enough that the thermal energy is small compared to the Fermi energy, i.e. the degeneracy parameter

$$\theta = \frac{k_B T}{E_F} = \frac{2m_e k_B T}{\hbar^2}(3\pi^2 n_e)^{-2/3}, \tag{1.2}$$

becomes small compared to 1. In degenerate plasmas nature of the particles becomes essential; their statistical behaviour is governed by the Fermi and the Bose statistics, respectively. For non-degenerate or classical plasma, $\theta >> 1$, the particles obey to the Boltzmann momentum distribution function.

A partially ionized dense hydrogen plasma is an object of this theoretical study, which focuses especially on the problem of interaction between electrons and hydrogen atoms.

Interactions of particles in dense plasma have a complex character, because even at moderate densities one should take into consideration collective effects such as the screening of the charge field in plasmas [Red97]. At high densities quantum effects play a essential role in interaction between partilces [RDO05].

1.2 Hydrogen

Hydrogen is the simplest of all chemical elements and the most abundant element in the Universe. Hydrogen and the second most abundant element, helium, together are about 98% of the mass of solar material [Lew04]. On Earth, it is the third most abundant element in the Earths surface, found in water and all organic matter. Hydrogen is of vast interest for the theoretical and experimental investigations because of its abundance in Universe and the simple electronic structure. The motivation of theoretical and experimental research on
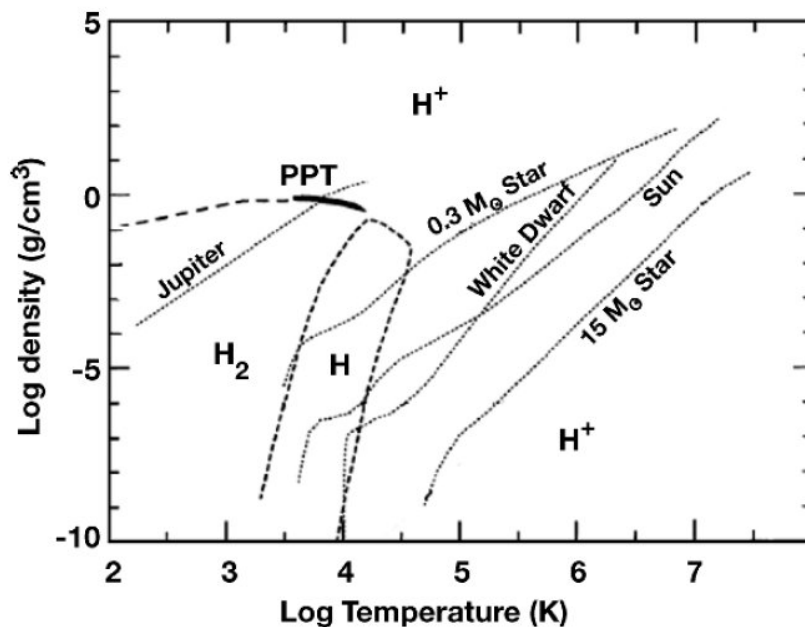
Figure 1.2: Phase diagram of hydrogen. Adapted from Ref.[SCWX00]

hydrogen is usually explained by interest in warm dense matter problems, applications to inertial confinement fusion research and to the interiors of giant planets, the hydrogen-rich planets, Jupiter and Saturn.

In Fig. 1.2 is presented a phase diagram for hydrogen, which was obtained in framework of a theoretical model based on the chemical picture [SCWX00]. At low densities with increasing of temperature, the molecular hydrogen dissociates into atomic hydrogen (at $T \sim 10^4$K), that then ionizes into ions (protons) (at $T \gtrsim 3 \cdot 10^4$K). At high pressures or high densities (at $\rho \sim 0.35$g/cm^3 of $T \sim 15000$K) of interesting phenomena such as

metallization of Hydrogen and the plasma phase transition (PPT) are expected. The plasma phase transition in hydrogen was predicted by Norman and Starostin [NS68], and Zeldovich and Landau [ZL44]. The existence of PPT in hydrogen has been investigated with different theoretical approaches and experiments. In Ref. [HNR07a] the summury of theoretical results for PPT in hydrogen was given. A review on studies of metal to nonmetal transitions can be found in Ref. [RHH10]. The Fig.1.2 shows also some astrophysical objects such as Jupiter, Sun, typical dwarf stars. One can see that pressure ionization of hydrogen is occured at these astrophysical objects.

Our understanding of the processes in the solar system depends on the properties of hydrogen, especially on the equation of state. The equation of state (EOS) is central interest in theoretical plasma physics since it is the basic thermodynamic quantity. It is also the key property to test the accuracy of different approaches to hot, dense hydrogen including analytical theories and numerical models. In this work the cluster-virial expansion is applied to calculate the EOS of a partially ionized hydrogen plasma, which consists of three components as electrons (e), ions (i) and hydrogen atoms (a). The formation of heavier clusters, such as molecules (H_2) or molecular ions (H_2^+), can also be included but is not considered here. To be specific, the results of the present work are presented at temperatures between $T = 5 \times 10^3$ K and $T = 2 \times 10^4$ K, and densities in the order of $n_e^{\text{total}} \leq 10^{22}$ cm^3 , where $n_e^{\text{total}} = n_e^{\text{free}} + n_e^{\text{bound}}$ is the total electron density including free and bound electrons. Such plasmas are nonideal and partially degenerate; the coupling parameter is $\Gamma \leq 0.9$, the degeneracy parameter is $\theta \geq 0.26$.

1.3 Equation of state

Of any of the topics in the plasma physics, investigations on equation of state constitute the area of greatest concern. This can be justified by an attempt to describe adequatly the plasma state and processes at a large range of temperature and number density. The equation of state gives us the phase diagramm of the plasma and provides us with our knowledge of the Sun, the stars, the interstellar medium and giant planets. Thus plasma science is related to astrophysical problems. The Sun has an average density of 1.4g/cm^{-3} , at the core of the Sun typically approaching a density of 150g/cm^{-3} and temperature of $1.571 * 10^7$K and the photosphere 10^{-7}g/cm^{-3} and 4000K, respectively [Rob], the parameters of the solar system planets are given in Ref.[htt]. The warm dense matter which satisfy to the state between normal condensed matter and the fully ionized plasma, has a great interest last decades. The hydrogen-helium equation of state were studied to describe the properties of the giant planets as Jupiter and Saturn [GSHS04, RHJ$^+$06a, Red05, LHR09, MC01, VSK04b]. Other direction of the hydrogen EOS investigations is connected with Inertial confinement fusion [LAB$^+$04]. Within the quantum statistical approach to the EOS, numerical techniques like density-functional (DFT) theory and quantum molecular dynamics (QMD) simulations have been elaborated [FSW08]. Several different numerical methods were developed in the past to describe thermodynamical properties of the nonideal plasma. We mention here the wave-packet

molecular-dynamics (WPMD) calculations and the path integral Monte Carlo (PIMC) simulations. The WPMD method was applied to the equation of state of hydrogen [KRTZ02] and deuterium [KRT01]. The results of the Ref.[KRT01] were compared with laser shock-wave experiments [SCCea97]. The laser shock wave experiments by Da Silva [SCCea97] and Collins et al.[Col98] are most relevant since they were the first direct measurements of the hydrogen equation of state in the megabar regime.

The theoretical methods, developed for calculation of the equation of state, are based on chemical or physical pictures. The chemical picture treats all components of plasma as separate species. This model is usefull for complicated system of plasma with constituents of free electrons, protons, ions, atoms and molecules. Though the chemical model is much more simple, especially for real plasmas, than the physical picture, but one should be carefull with double counting of effects. The chemical models or the free energy models currently used to predict properties of hydrogen employ elaborate schemes to determine the interaction terms. Not all of them were constructed to describe the whole high temperature phase diagram as done by Saumon and Chabrier [SC92]. Ebeling [ER5b] studied the plasma and the atomic regime, while models by Beule et al. [BEF99] and Bunker et al. [BNRR97] were designed to the describe the dissociation transition. The Ross [Ros98] model was primarily developed to study the molecular-metallic transition.

The physical picture where one treats the fundamental particles, in this case electrons and proton, individually and compound particles such as atoms and molecules are formed if the fundamental particle are bound together. The physical picture refers to approaches based on many-body fugacity expansions of the grand canonical partition function [EKK77, KSK05, WDWG86, Rog84]. This approach deals with the pure Coulomb interaction between electrons and nuclei. Consequently, masses, charges and abundancies of nuclei are only input of the theory. The description of the pressure ionization phenomenon can be provided by the physical picture. As well known, in the chemical picture one difficulty is how to treat the interaction of charged and neutral particles. Often, this is done by introducing hard-sphere radii (excluded volume concept) and additional corrections [EFF$^+$91, RHJ$^+$06a]. The main point of the excluded volume concept is the consideration of atoms as a hard sphere. The volume which is taken by atoms cannot be penetrated by the charged particles. In this case the free energy depends on the effective volume $V^* = V(1 - \eta) = V - V_{HS}$, where V_{HS} is the volume occupied by atoms, $\eta = V_{HS}/V$ is the filling parameter.

The effects of plasma environment on bound states, formation of bound states and transit to scattering states can be described due to the Beth and Uhlenbeck formula [BU37] for the second virial coefficient. Calculation of the second virial coefficient by Beth-Uhlenbeck formula gives a possibility to observe the formation or disappearance of the bound states and its influence on the thermodynamics of the system. In particular, we look at the electron-atom pairs, since the second virial coefficient for the charged particles was already evaluated [WDWG86].

1.4 Interactions in a partially-ionized plasma

The interaction of particles is one of the main problems in calculating the physical properties of plasma, such as thermodynamical, transport and optical properties. It is known that the form of the interaction potential plays an important role to obtain accurate data calculating such properties. In particular, many-particle effects have to be considered in dense plasmas such as collective modes, strong collisions and quantum effects. Among the various systems of interacting particles, systems of charged particles reveal particular properties due to the long-range character of interaction. Previously, the theoretical consideration of plasma frequently required one to overcome difficulties with the Coulomb potential divergence at large and short distances

$$V_{cd}(r) = \frac{Z_c Z_d \, . e^2}{r},$$ (1.3)

Still, this potential is a long-range one and particle collisions in plasma are different from particle collisions in such neutral media as liquids or gas; a characteristic feature is that particles scatter in plasma at low angles and change in their momentum is small. That is why the main contribution to the collision integral is provided by particle scattering at large impact parameters.

The presence of surrounding charged particles and their collective interactions result in screening of the microscopic interaction potential. In the linear approach with effective interaction potential for charged particles that takes into account such screening, there is the well-known potential of Debye-Hückel for c, d species of particles:

$$V_{cd}(r) = \frac{Z_c Z_d e^2}{r} e^{-r/r_D},$$ (1.4)

where $r_D = [\epsilon_0 \, k_{\mathrm{B}} T / \sum_c n_c e^2]^{1/2}$ is the Debye screening radius. The Debye-Hückel potential corresponds to the approximation of pair correlations in the interaction of charged particles.

Considerable attention has to be paid to interaction of particles of semiclassical plasmas. At high densities and temperatures quantum effects play essential role and their consideration within specific region is just necessary. Quantum-mechanical diffraction effects are well-described by unscreened potential of Kelbg-Deutsch-Yukhnovskiy [Kel63, GY52, DFG81, Deu77]:

$$V_{cd}(r) = \frac{Z_c Z_d e^2}{r} (1 - e^{-r/\Lambda_{cd}}),$$ (1.5)

where $\Lambda_{cd} = (2\pi\hbar^2/k_{\mathrm{B}}T m_{cd})^{1/2}$ denotes the thermal wavelength of species c, and $n_c = N_c/V$ the particle number density of the components c, d.

The interaction of charged particles (electrons) with atoms differs from the interaction of charged particle drastically. The main two effects in interaction of electron with atom can be pointed out as polarization and exchange effects. At large distances the interaction between an isolated atom and a charged particle has a polarization character $\alpha e^2/2r^4$ with

α a polarizability of the atom. However, this potential is not appropriate for dense plasmas. At short distances, it becomes singular. To avoid singularity and to include plasma effects, polarization pseudopotential models were eloborated. The Buckingham model, which includes the screening effects and cutoff radius, is often used to describe electron-atom interaction in calculations of the transport and thermodynamical properties of dense partially ionized plasma. E.g. in Refs.[KR00, RGD⁺03] this model was applied to study transport properties of partially-ionized plasma. The conductivity of inert gas and metal plasma was calculated in Ref.[KR00] and for Cesium in Ref. [RGD⁺03]. The quantum effects as well as screening effects are taken into account in the model in Ref.[RDO05]. This model was applied in the calculation of the elastic scattering processes [RDOR07, WSY07] and the thermodynamics of the metal plasmas [RDG⁺09].

1.5 The aim and structure of this work

As it was mentioned in Sec. 1.3 the terms "chemical picture" and "physical picture" are popular concepts for approaches in calculations of the EOS of partially-ionized plasma. The chemical picture is based on the assumption that free energy is separable for every species of a partially-ionized plasma. It means that the species of plasma considered remain chemically distinct under all conditions. The many-body effects are absorbed in an effective pair potential. The physical picture is based on first-principal approaches consider only electrons and nuclei, example of such physical picture is the fugacity expansion. In this picture pressure and density are given by the fugacity expansion. Formation of bound states can be automatically included in the fugacity expansion. In low density limit two-particle bound states are stable. Therefore it is possible to consider the bound states as a new particles. It means we switch from the physical picture to the chemical picture. In partially- ionized hydrogen plasma with three components, electrons e, protons i, atoms a, the formation of negative hydrogen ion H^- leads to four component system, if we consider H^- as a new particle. The second virial coefficient b_{ea} includes bound and scattering states by the formula of Beth and Uhlenbeck $b_{ea} = b_{ea}^{\text{bound}} + b_{ea}^{\text{sc}}$. The first term represents the contribution of three-particle bound states to the pressure, i.e. it accounts H^--particles. The second term gives the contribution of scattering states. The aim of this work is taking into account an influence of the electron-atom interaction on the thermodynamical properties of a partially-ionized hydrogen plasma by systematically way using the quantum statistical approach. The contribution of electron-atom interaction to the EOS is calculated using the Beth-Uhlenbeck formula [BU37, Hua66, SRS90] for the second virial coefficient. Calculation of the second virial coefficient by Beth-Uhlenbeck formula gives a possibility to observe the formation or disappearance of the bound states and its influence on the thermodynamics of the system. In particular, we look at the electron-atom pair, since the second virial coefficient for the charged particles was already evaluated [WDWG86]. The formation of heavier particles is neglected.

    This work is organized as follows. Chapter 2 starts with a consideration of the chemical picture and the nonideality correction that will be used throughout this work. Chapter

3 considers electron-atom interaction models, such as Buckengham and RDO polarization models and rank two and one separable potentials. The phase shifts of electron-atom scattering which is needed to calculate the second virial coefficient are found in chapter 4. Some results of the scattering cross section of electrons on atoms calculated on the basis of interaction models are given in Sec. 4.4. In chapter 5, we present density virial expansions as well as fugasity cluster virial expansion and the virial expansions for the thermodynamical functions. Switch from the physical picture to the chemical picture is also shown in this chapter. The Beth-Uhlenbeck formula for the second virial coefficient of electron-atom interaction is given in Sec. 5.2.3. Results for the second virial coefficient of atom-atom and electron-atom contributions are presented in chapter 6. Comparison of the excluded volume concept with cluster virial approach is performed also in this chapter 6. Results of the generelized Beth -Uhlenbeck approach which considers the Pauli blocking effect are presented in section 6.4. Finally, the main results are summerized in conclusions.

Chapter 2

Partially ionized plasma and the chemical picture

2.1 Ideal mixture

The theoretical methods, developed for calculation of the equation of state, are based on chemical or physical pictures. The chemical picture treats all components of plasma as separate species. This model is usefull for complicated system such as a plasma with constituents of free electrons (e), ions (p, H^-, H_2^+), atoms (H) and molecules (H_2). Study of the thermodynamics in the framework of the chemical model makes it possible to consider the contribution of each species to the total thermodynamical function separately.

A mixture of neutral (H, H_2) and charged (e, i, H^-) components is in chemical equilibrium refering to dissociation and ionization. The dissociation ($H_2 \rightleftharpoons 2H$) and ionization (e.g. $e + p \rightleftharpoons H$ and $e + H \rightleftharpoons H^-$) processes can be taken into account due to the mass action law. For simplicity we consider further the free electrons (e), free ions (protons, i), atoms (a) and the formation of other species (H_2, H^-, H_2^+) will be neglected. The mass action law $\mu_e + \mu_i = \mu_a$ in chemical equilibrium defines the degree of ionization. If we consider an ideal mixture i.e. the interaction between the components is neglected, the degree of ionization $\alpha = n_e/n_e^{\text{tot}}$ can be obtained from the ideal Saha equation [LL88]:

$$\frac{1 - \alpha}{\alpha^2} = n_e^{\text{tot}} \Lambda_e^3 \exp\left[\beta I_{\text{id}}^{\text{eff}}(n_e, T)\right] \ , \tag{2.1}$$

where the total number density of electrons is $n_e^{\text{tot}} = n_e + n_a$, the total number density of ions due to electron neutrality is $n_i^{\text{tot}} = n_i + n_a = n_e^{\text{tot}}$. The ionization potential is equal to the bound state energy of isolated atom $I_{\text{id}}^{\text{eff}}(n_e, T) = |E_a^0|$. The ideal mixture approximation can be extended including molecules at ground state. This simple calculation is usefull to describe thermodynamics of low temperature gaseous plasma. Fig. 2.1 presents the degree of ionization for the ideal mixture in dependence on temperature and density number.
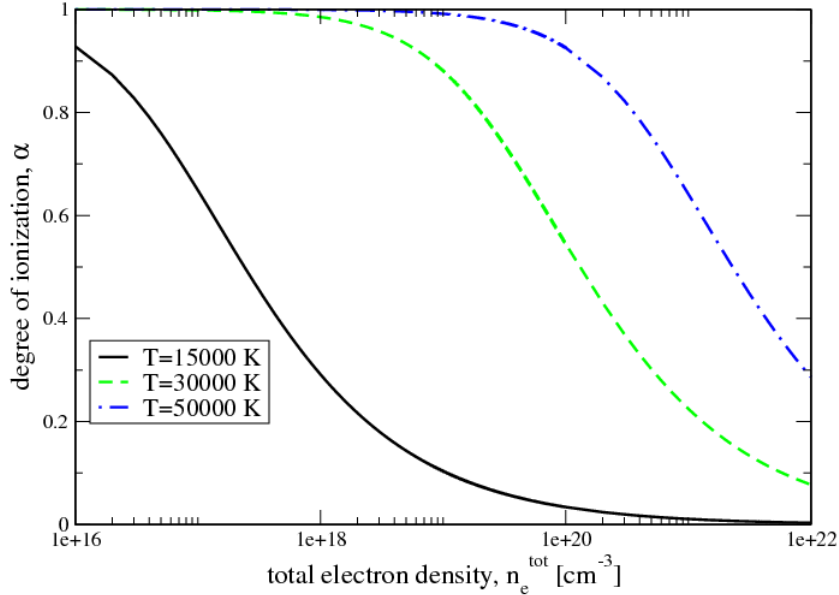
Figure 2.1: Degree of ionization of the ideal mixture as a function of the total electron density for three different temperatures, $T = 1.5, 2, 3 \cdot 10^4$ K.

2.2   Nonideality corrections

The different theoretical methods were developed to calculate the nonideal corrections to the thermodynamic functions. The influence of the nonideal effects can be taken into account due to the adequate interaction models of free charged particles, methods of limiting the atomic statistical sum or interaction models for neutral particles if there occurs dissociation process. The nonideal part of thermodynamical functions for the interacting system of electrons, ions and atoms represents the sum of the contributions of $e - e$, $e - i$, $e - i$, $e - a$, $i - a$, and $a - a$ interactions. If for the contributions of the free charged particles it is enough to use pseudopotential model, for neutral components it is necessary to consider also internal, excited states of the atom.

In a multicomponent plasma the total free energy calculations start from a linear-mixing expression. E.g. in Refs.[SJR05, HNR07b, RHJ$^+$06b] the free energy was defined as $F = F_0 + F_\pm + F_{\rm pol}$, assuming the linear mixing between neutral (F_0) and charged particles ($F_\pm$), the $F_{\rm pol}$ describes the polarization interaction between charged and neutral particles. Fluid variational theory (FVT) was applyed to calculate the F_0 and the Pade approximation for $F_\pm$ [CP98]. The EOS were derived using the the free energy minimization technique.

The nonideal corrections to the pressure takes the form [VSK04a] $P = p_{\rm id} + p_{\rm HF} + p_{\rm MW} + \mathcal{O}(e^4)$. Here $p_{\rm id}$ is the ideal part, $p_{\rm HF}$ is the Hartree-Fock term, describing the mean

field Coulomb and exchange contribution, and p_{MW} is the Montroll-Ward contribution, containing the dynamically screened self-energy. The ionization energy shifts due to the influence of the surrounding plasma

$$I^{\text{eff}}(n_e^{\text{tot}}, T) = |E_a^0| - \Delta_a + \Delta_e + \Delta_i \qquad (2.2)$$

depend on density and temperature. The interaction contributions Δ_c (energy shift) of the particles are included in the effective ionization energy. The energy shifts can be calculated from the Schrödinger equation with the effective Hamiltonian. Inthe simplest approximation the energy shift for charge particles $\Delta_e = \Delta_i = -\frac{\kappa e^2}{2}$ is derived applying the Debye-Hückel potential (1.4). $\kappa = [n_e^{\text{free}} e^2 / \epsilon_0 \, k_{\text{B}} T]^{1/2}$ is the inverse Debye screening length. As an approximation it can be taken $E_1^0 = -\frac{e^2}{2a_B}$, the ground state energy of the Hydrogen atom. The effective ionization potential vanishes with the increasing of the density. At the point $I^{\text{eff}}(n_e^{\text{tot}}, T) = 0$ the degree of ionization changes drastically, the bound states merges into scattering state. This represents pressure ionization and called as *Mott effect.* .

2.3   Chemical and physical picture

The alternative model is the physical picture. This model deals with electrons and nuclei and other components, as ions, atoms and molecules, build from electrons and nuclei. Starting from canonical ensemble one can derive a virial dencity expansion for the EoS in the physical picture, from the grand canonical expression - fugacity expansion. The "physical picture" is quite successful at relativly low densities, become complicated at high densities. The cluster-virial expansion represents a "chemical" picture in the sense that the virial is expanded in orders of the fugacities of the different components (single-particle states, bound states) in the system. In contrast, the traditional virial expansion is a "physical" picture, i.e. the fugacities of elementary particles, such as electrons and nuclei in the case of ionic plasmas, are the expansion variables. In the physical picture, bound states appear in higher order virial coefficients. The treatment of the latter involves sophisticated mathematics. On the other hand, bound states are naturally included already in the lowest order of the chemical picture. For special parameter values, bound state formation gives the leading contribution, e.g. in atomic or molecular gases. The chemical picture accounts for these main terms already in the lowest order of the virial expansion, whereas within the physical picture we have to consider higher orders of the expansion to identify the leading contributions.

Chapter 3

Interaction of electrons with atoms

3.1 Polarization pseudopotential models

One of the advantages of introducing pseudopotentials is the possibility to describe medium effects such as screening and quantum degeneracy. Polarization effects at long distances and exchange effects at short distances play a key role in the $e - a$ interaction in a dense plasma. Below we use polarization potential models, which include these many-body features to calculate the scattering phase-shifts. Of course, the introduction of a local and instant pseudopotential for the $e - a$ interaction is only an approximation. A rigorous treatment involves the three-particle T matrix, which is non-local due to exchange effects and depends on energy. We do not describe this problem in detail here.

As well known, at large distances the interaction between an isolated atom and a charged particle is given by:

$$V_{ea}(r) = -\frac{\alpha e^2}{2r^4},$$

(3.1)

where $\alpha = 4.5\,a_{\rm B}^3$ is the hydrogen atom polarizability (here and henceforth we measure distances in units of the Bohr radius, $a_{\rm B} = 0.529\,\text{Å}$). The polarization potential (3.1) has a long-range nature, in comparison with exchange effect, which drop off exponentially for large r. However, this potential is not appropriate for dense plasmas. At short distances, it becomes singular. It has to be modified if r is of the order of the extension of the atom as given by the Bohr radius a_B. According to Buckingham, a cutoff radius r_0 can be introduced leading to the potential

$$V_{ea}(r) = -\frac{\alpha e^2}{2(r^2 + r_0^2)^2} \,,$$

(3.2)

The cutoff radius r_0 is used to regularize the behaviour at small distances. Its value given in the literature [Red97] is $r_0 = 1.4565\,a_{\rm B}$. However, we suggest here the use of a different value $r_0 = 1.033\,a_{\rm B}$, which yields the correct H^- ion ground state energy $E_0 = -0.7542\,\text{eV}$ as the eigenvalue of the effective radial Schrödinger equation [WDWG86]. At large distances $r \gg r_0$ the Buckingham potential describes the typical $1/r^4$ behaviour of the electron potential energy in the field of the polarizable H-atom.

For comparison, we give also the Buckingham screened electron-atom potential model, which was often used for the investigation of properties of partially ionized hydrogen plasmas [KR00, RGD$^+$03]. Redmer and et al. [Red97] found the expression

$$V_{ea}(r) = -\frac{e^2\alpha}{2(r^2 + r_0^2)^2} \exp\left(-\frac{2r}{r_D}\right)(1 + \frac{r}{r_D})^2. \tag{3.3}$$

Finally we use an effective polarization potential for partially ionized dense plasma which was proposed by Ramazanov and et al [RDO05]. This model takes into account quantum-mechanical as well as screening effects

$$V_{ea}(r) = -\frac{e^2\alpha}{2r^4(1 - 4\lambda_e^2/r_D^2)} \times \left(e^{-Br}(1 + Br) - e^{-Ar}(1 + Ar)\right)^2, \tag{3.4}$$

where $A^2 = (1 + \sqrt{1 - 4\lambda_e^2/r_D^2})/(2\lambda_e^2)$, $B^2 = (1 - \sqrt{1 - 4\lambda_e^2/r_D^2})/(2\lambda_e^2)$, and $\lambda_e = \Lambda_e/2\pi$ is the electron thermal de Broglie wave-length. This model depends on two parameters λ_e and r_D. The strength of the model at short distances is given by $-\alpha e^2/8\lambda_e^4$. Fixing $r_D = 4.84\,a_B$ and $\lambda_e = 0.62\,a_B$, the H$^-$ ground state energy is found at the correct energy. The different
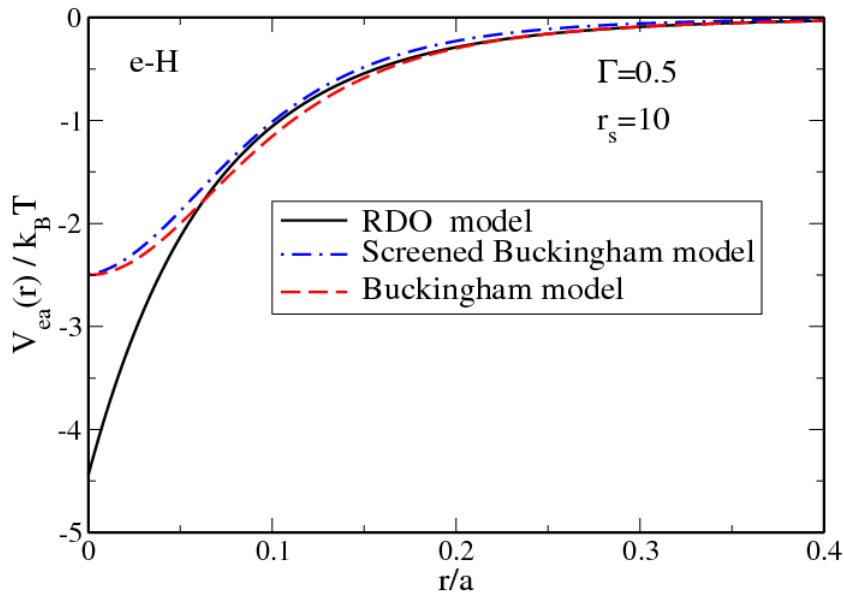

Figure 3.1: Effective polarization potentials for the electron- atom interaction in hydrogen plasmas at $\Gamma = 0.5$ and $r_s = 10$. Full line - Eq. (3.4), dot-dashed- Eq.(3.2), dashed - Eq. (3.1).

electron-atom pseudopotentials (3.1), (3.2) and (3.4) are presented in Fig. 3.1 for plasma parameters $\Gamma = 0.5$, $r_s = 10$. In the low-density limit $r_D \to \infty$ we find the limiting

behavior of the polarization potential (3.4) as $V_{ea}(r) \rightarrow e^2\alpha(1\exp r/\lambda_e(1 + r/\lambda_e))^2/2r^4$ and the Buckingham potential (3.2) as $V_{ea}(r) \rightarrow e^2\alpha/2(r^2 + r_0^2)^2$. In the limit $r \rightarrow 0$ the potential (3.4) has a finite value $V_{ea}(0) \rightarrow e^2\alpha/8\lambda_e^4$ which depends on the temperature of the system. The Buckingham potential (3.2) has also a finite limiting value $V_{ea}(0) \rightarrow e^2\alpha/2r_0^4$ which however, does not depend on the plasma parameters.

The short range behavior of the effective interaction between the atom and an electron needs more detailed consideration. In principle, we have to consider two possibilities for the spin orientations of the electrons. If the spins of the free as well as the bound electrons are parallel, due to the Pauli exclusion principle we have a strong repulsion at short distances. However, neither the Buckingham model, Eq. (3.1), nor the RDO model, Eq. (3.4), take into account this exchange effect. A convenient method to overcome this problem consists in using a separable potential [Mon69, Yam54]. This will be discussed in the following section 3.2.

3.2   Separable potential method

Separable potentials have been used extensively in nuclear physics to parametrize the nucleon-nucleon interaction [Mon69]. It can be shown that any interaction potential can be approximated by a sum of separable potentials [EST73].

We characterize different channels by spin and angular momentum and assume that there is no coupling between different channels. We consider a rank-two separable potential in momentum representation to describe attraction at long distances and repulsion at short distances,

$$V(p, p') = \lambda_1 w_1(p)w_1(p') + \lambda_2 w_2(p)w_2(p') \tag{3.5}$$

where $w_1(p)$, $w_2(p)$ are Gaussian form factors $w_i(p) = \exp\left(-p^2/b_i^2\right)$, and λ_i, b_i are the strength and interaction range, respectively. We determine these parameters by fitting the phase-shifts obtained from the separable potential to the experimental data. Thereby we exploit the definition of the phase-shifts as the argument of the T-matrix,

$$\tan\eta(p) = \frac{\Im T(p, p', \frac{p^2}{2m_r})}{\Re T(p, p', \frac{p^2}{2m_r})}, \tag{3.6}$$

We consider the low density limit $n_e\Lambda_e^3 \ll 1$, where the T-matrix equation [LS50] for a separable potential reads:

$$T(p, p', E) = V(p, p') + \sum_{p''} V(p, p'')\frac{1}{\frac{p''^2}{2m_r} - E}T(p'', p', E). \tag{3.7}$$

For the rank-two separable potential (3.5), we obtain the following expression for the T-

matrix:

$$
\begin{aligned}
T(p, p', E) &= \lambda_1 w_1(p)w_1(p') + \lambda_2 w_2(p)w_2(p') + \lambda_1 w_1(p) \int \frac{d^3 p''}{(2\pi)^3} w_1(p'') \frac{1}{\frac{p''^2}{2m_r} - E} T(p'', p', E) \\
&\quad + \lambda_2 w_2(p) \int \frac{d^3 p''}{(2\pi)^3} w_2(p'') \frac{1}{\frac{p''^2}{2m_r} - E} T(p'', p', E) \\
&= c_{11} w_1(p)w_1(p') + c_{22} w_2(p)w_2(p') + c_{12} w_1(p)w_2(p') + c_{21} w_2(p)w_1(p'), \quad (3.8)
\end{aligned}
$$

with

$$
c_{ij} = \lambda_i \delta_{ij} + \lambda_i \int \frac{d^3 p''}{(2\pi)^3} w_i(p'') \frac{1}{\frac{p''^2}{2m_r} - E} (c_{1j} w_1(p'') + c_{2j} w_2(p'')) \quad (3.9)
$$

This set of equations can be simplified if we introduce the integrals

$I_{ij}(E) = \int \frac{d^3 p''}{(2\pi)^3} \frac{1}{\frac{p''^2}{2m_r} - E} c_{ij} w_i(p'') w_j(p'')$:

$$
c_{ij} = \lambda_i \delta_{ij} + \lambda_i I_{i1}(E) c_{1j} + \lambda_i I_{i2}(E) c_{2j} \quad (3.10)
$$

Finally, after some mathematics, we obtain the T-matrix in the following form:

$$
\begin{aligned}
T(p, p', E) &= \frac{1}{\text{Det}(E)} \Big\{ \big(\lambda_1 \big[1 - \lambda_2 I_{22}(E)\big] w_1(p)w_1(p') \\
&\quad + \lambda_2 \big[1 - \lambda_1 I_{11}(E)\big] w_2(p)w_2(p') + \lambda_1 \lambda_2 I_{12}(E) w_1(p)w_2(p') \\
&\quad + \lambda_1 \lambda_2 I_{21}(E) w_2(p)w_1(p') \Big\} \quad (3.11)
\end{aligned}
$$

where the determinant is

$$
\text{Det}(E) = \big[1 - \lambda_1 I_{11}(E)\big]\big[1 - \lambda_2 I_{22}(E)\big] - \lambda_1 \lambda_2 I_{12}(E) I_{21}(E). \quad (3.12)
$$

Using properties of the T-matrix, the binding energy E_0 can be obtained from the equation $\text{Det}(E_0) = 0$.

Fig. 4.3 shows the phase-shifts for the singlet and triplet scattering channels obtained by the separable potential in comparison with data of Ref. [Sch61]. The best fit parameters are summarized in Tab. 3.1. Column 4, 5 and 6 give the scattering length a and the effective range R from the effective radius theory, and the binding energy E_0 used to fix two of the parameters λ_i and b_i, the remaining two being fixed directly by comparison to the experimental phase-shifts. The effective radius theory was applied e.g. in Ref. [SR10] to calculate the influence of atomic and molecular contributions to the EOS of hydrogen plasma. However, the effective radius theory is limited to s-wave scattering, and therefore to low energies. Furthermore, in Ref. [SR10], the spin dependence of the $e-a$ interaction is neglected. The two-rank separable potential for both singlet and triplet states is presented at the Fig. 3.2. As we can see the singlet separable potential has a attractive character

Table 3.1: Parameters of the rank-two and rank-one separable potentials (λ_1, λ_2, in Hartree, and b_1, b_2 in a_B), the scattering length (a), the effective range (R), the binding energy (E_0) for the singlet ($S = 0$) and the triplet ($S = 1$) channels of s-wave.

	λ_1	λ_2	b_1	b_2	a/a_B	R/a_B	E_0, Hartree
	rank-two separable potential						
$S = 0$	-25.4	10	0.8	0.787	5.965	$-$	-0.06899
$S = 1$	37	40	0.8	0.787	1.97	$-$	$-$
	rank-one separable potential						
$S = 0$	-45.4	0	0.4705	0	5.965	3.32	-0.0474
$S = 1$	77.67	0	0.9	0	1.77	1.1	$-$
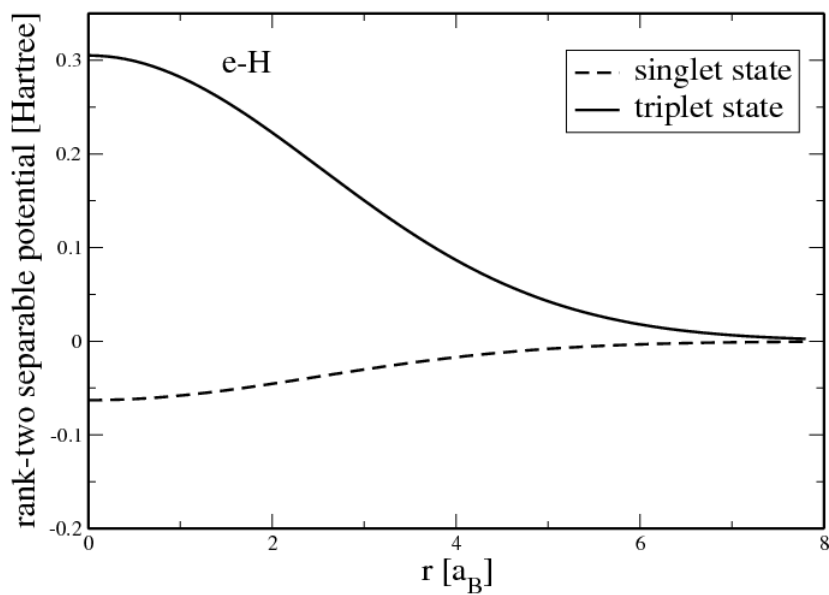
Figure 3.2: Singlet and triplet two-rank separable potentials for interaction of electron with hydrogen atom. The parameters of the separable model are given in the Tab. 3.1.

and triplet one negativ. At this point we want to remark that the bound state occurs only in the singlet scattering channel.

Choosing $\lambda_2 = 0$ and $b_2 = 0$ in Eq. (3.5), a rank-one separable potential is obtained. Parameters of a rank-one separable potential are given in the Tab. 3.1 (bottom part). Using the properties of the T-matrix (see Refs. [?, WDWG86]), we found the binding energy E_0 of the H^- ion for both versions of the separable potentials, given in the last column of Tab. 3.1. The experimental value of the binding energy is $E_0 = -0.0277$ Hartree ($-0.7542\,\text{eV}$) [MW74]. The two-particle properties, i.e. scattering phase-shifts and the bound state properties, can be reproduced in certain approximation by separable potentials. We expect that increasing the rank of the potential, the experimental values for the two-particle properties are better realized.

Chapter 4

Elastic scattering of electrons on hydrogen atoms

4.0.1 Experimental data and first-principle calculations

The Beth-Uhlenbeck formula relates the second virial coefficient to few-body properties. For the electron-atom contribution, the relevant quantities are the phase-shifts for the elastic electron-atom scattering as well as the possible bound state energies. No direct measurements of the electron-atom scattering phase-shift are available in the literature, only scattering cross-sections (i.e. the modulus of the phase-shift) have been measured. Accurate data for the angular resolved scattering cross-section were obtained by Williams *et al.* [Wil75] for electron energies between $0.58\,\mathrm{eV}$ and $8.7\,\mathrm{eV}$ and by Gilbody *et al.* [GSF61] for $3.4\,\mathrm{eV}$, see the review in Ref. [Wil98]. The data are shown in Figs. 4.1 and 4.2.

A bound state H^- is measured at energy $(0.754 \pm 0.002)\,\mathrm{eV}$ [MW74]. In this measurement, the electron affinity was obtained via the threshold energy for photodissociative formation of ion pairs from H_2 [MW74]. The ion pair threshold was combined with the ionization potential of the hydrogen atom and the bound dissociation energy of H_2 to obtain a lower bound to the electron affinity. This results is in agreement with the theoretical value of $0.75421\,\mathrm{eV}$ reported by Pekeris [Pek62] for the singlet bound state of H^-.

Theoretical calculations for the $e - a$ scattering phase-shifts are abundant. The spins of the two electrons are combined to a singlet or triplet state, whereas the orbitals are determined by a three-body Schrödinger equation and the symmetry condition for fermions. Frequently used methods are the close-coupling approximation [BSW67], the R-matrix method [SSB88], direct numerical solution of the Schrödinger equation [WC93], the wave expansion method [F.C67, Bab76], and variational calculations. Using the variational method, Schwartz *et al.* [Sch61] obtained the phase-shifts for the s-waves (orbital momentum $\ell = 0$ of the $e - a$ system) in the singlet and triplet channels. For higher orbital moments $\ell = 1, 2$ calculations have been performed by Armstaed [Arm68] and Register [RP75]. Comparing the experimental data with results of numerous theoretical approaches, see Refs [Wil75, RP75, FWE$^+$07], it was concluded that the variational approach is the
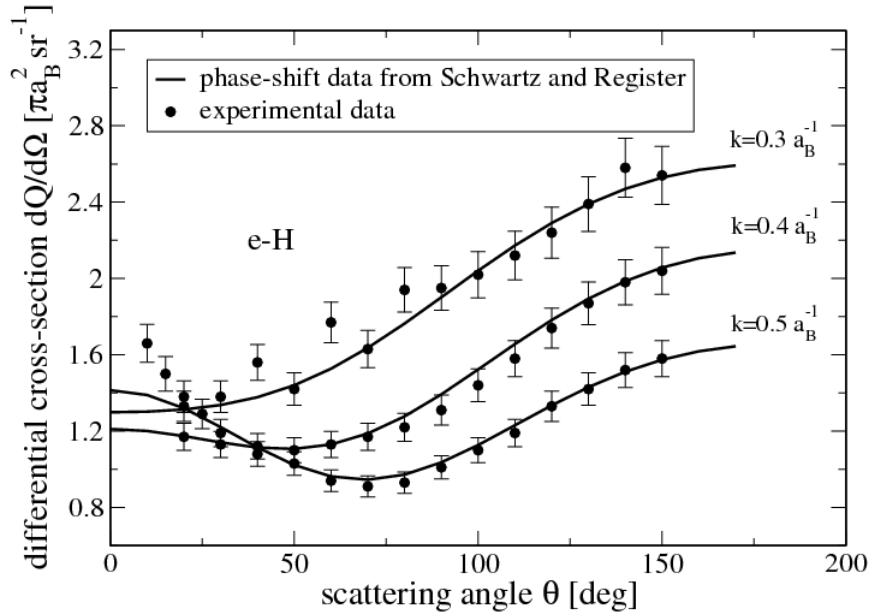
Figure 4.1: Differential scattering cross-section of electrons on atoms (e-H) as a function of the scattering angle for electron wavenumber $k = 0.3 \ a_B^{-1}$, $k = 0.4 \ a_B^{-1}$, $k = 0.5 \ a_B^{-1}$; solid lines - phase-shift data from the variational method [Sch61, RP75], circles - experimental data [Wil75].

most reliable and most accurate method in reproducing the experimental scattering cross-sections.

In Figs. 4.1 and 4.2 we show the differential cross-section as calculated from the phase-shifts given in Refs [Sch61, RP75] compared to the experimental data from Ref. [Wil75]. Good agreement between theory and experiment is observed for scattering angles larger than $\theta \simeq 25°$. Deviations below $25°$ are due to the neglect of higher orbital momenta $\ell > 2$ in the variational calculations [Wil75].

4.1   Wave expansion method

Let us consider scattering of spinless particle with defined energy values k^2 and orbital moment ℓ by a spherically symmetrical potential $U_{cd}(r)$. The Schrödinger equation for radial component of the wavefunction $u_\ell(r)$ takes the following form:

$$\frac{d^2}{dr^2}u_\ell(r) + [k^2 - \frac{\ell(\ell+1)}{r^2} - U_{cd}(r)]u_\ell(r) = 0 \tag{4.1}$$

Two linearly independent real solutions for the free ($U_{cd}(r) = 0$) equation (4.1) are the
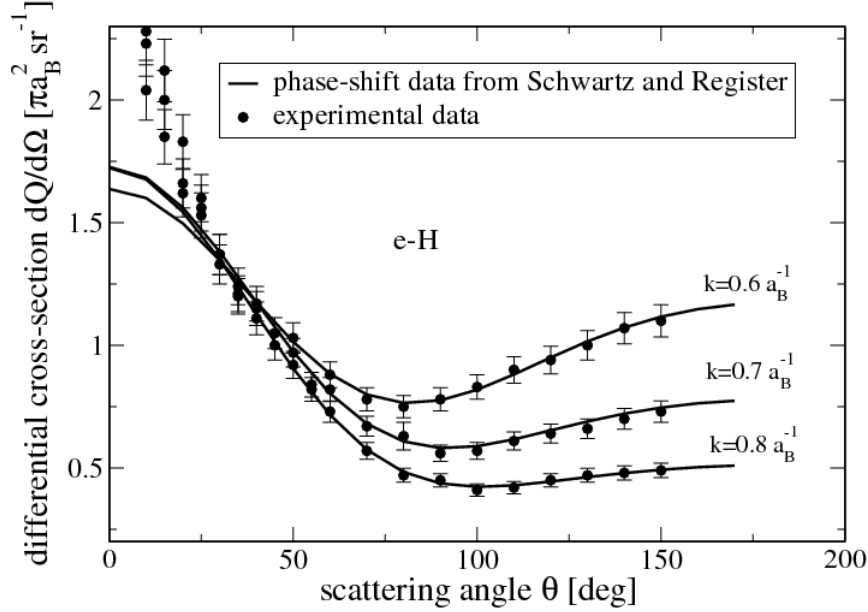
Figure 4.2: The same as in Fig. 4.1 for $k = 0.6\ a_B^{-1}$, $k = 0.7\ a_B^{-1}$, $k = 0.8\ a_B^{-1}$.

known Ricatti-Bessel functions $j_\ell(kr)$ and $n_\ell(kr)$ [AS64].

The presence of the potential results in the additional irregular solution $n_\ell(kr)$ in the wavefunction of the free equation in the region where $U_{cd}(r)$ disappears. The measure of this contribution for the quantitative description of the interaction is the scattering phase η_ℓ^{cd}:

$$u_\ell(r) = const[j_\ell(kr) - \tan\eta_\ell^{cd}n_\ell(kr)], \tag{4.2}$$

$$u_\ell(r) = const\sin(kr - \frac{\ell\pi}{2} + \eta_\ell^{cd}), \quad r \to \infty. \tag{4.3}$$

A set of phase shifts η_ℓ^{cd} for various partial waves ℓ determines the angular distribution and total scattering. That is why an important task in the theory of potential scattering is to determine η_ℓ^{cd} values at given potential $U_{cd}(r)$, orbital moments ℓ and k^2. The method of phase functions means the transition from Schrödinger equation to an equation for the scattering phase. To this end, let us introduce two new functions $\eta_\ell^{cd}(r)$, $A_\ell^{cd}(r)$ as:

$$u_\ell(r) = A_\ell^{cd}(r)[\cos\eta_\ell^{cd}(r)j_\ell(kr) - \sin\eta_\ell^{cd}(r)n_\ell(kr)] \tag{4.4}$$

The physical meaning of the functions $\eta_\ell^{cd}(r)$, $A_\ell^{cd}(r)$ can be clarified with some additional conditions imposed on them. Therefore let the following condition be satisfied for an arbitrary wavefunction:

$$\frac{d}{dr}u_\ell(r) = A_\ell^{cd}(r)[\cos\eta_\ell^{cd}(r)\frac{d}{dr}j_\ell(kr) - \sin\eta_\ell^{cd}(r)\frac{d}{dr}n_\ell(kr)] \tag{4.5}$$

Equivalent to the additional condition

$$\frac{dA_\ell^{cd}(r)}{dr}[\cos\eta_\ell^{cd}(r)j_\ell(kr) - \sin\eta_\ell^{cd}(r)n_\ell(kr)] - \frac{d\eta_\ell^{cd}(r)}{dr}A_\ell[\cos\eta_\ell^{cd}(r)j_\ell(kr) - \sin\eta_\ell^{cd}(r)n_\ell(kr)] = 0 \tag{4.6}$$

Comparing (4.2) and (4.4) one can see that if the potential is "cut" above some point $r = R$:

$$U_{cd}(r, R) = U_{cd}(r)\theta(R - r), \quad \theta(x > 0) = 1, \quad \theta(x \leqslant 0) = 0 \tag{4.7}$$

then in the region $r > R$ the functions $\eta_\ell^{cd}(r)$, $A_\ell^{cd}(r)$ have constant values η_ℓ^{cd}, A_ℓ^{cd} equal to the scattering phase and amplitude of the asymptotic expression for the wavefunction. The functions $\eta_\ell^{cd}(r)$, $A_\ell^{cd}(r)$ are called by their physical meaning as the phase and amplitude functions. Upon differentiation of (4.5) let us use the expression $d^2u_\ell(r)/dr^2$ together with (4.4) in the Schrödinger equation (4.1):

$$\frac{dA_\ell^{cd}(r)}{dr}\Big[\cos\eta_\ell^{cd}(r)\frac{d}{dr}j_\ell(kr) - \sin\eta_\ell^{cd}(r)\frac{d}{dr}n_\ell(kr)\Big]$$
$$-\frac{d\eta_\ell^{cd}(r)}{dr}A_\ell^{cd}(r)\Big[\sin\eta_\ell^{cd}(r)\frac{d}{dr}j_\ell(kr) - \cos\eta_\ell^{cd}(r)\frac{d}{dr}n_\ell(kr)\Big]$$
$$-U_{cd}(r)A_\ell^{cd}(r)[\cos\eta_\ell(r)j_\ell(kr) - \sin\eta_\ell^{cd}(r)n_\ell(kr)] = 0. \tag{4.8}$$

Equations (4.6) and (4.8) form a system of two differential equations of the first order for $\eta_\ell^{cd}(r)$, $A_\ell^{cd}(r)$. Excluding the derivative of the amplitude function and taking the Vronskian of solutions for a free Schrödinger equation as:

$$j_\ell(kr)\frac{d}{dr}n_\ell(kr) - n_\ell(kr)\frac{d}{dr}j_\ell(kr) = k \tag{4.9}$$

We get the following equation for the phase functions, which is now depends also on k - $\eta_\ell(k, r)$:

$$\frac{d}{dr}\eta_\ell^{cd}(k, r) = -\frac{1}{k}U_{cd}(r)\Big[\cos\eta_\ell^{cd}(k, r)j_\ell(kr) - \sin\eta_\ell^{cd}(k, r)n_\ell(kr)\Big]^2. \tag{4.10}$$

where $U_{cd}(r) = \frac{2\mu_{cd}}{\hbar^2}V_{cd}(r)$, $V_{cd}(r)$ is the interaction potential and μ_{cd} is the reduced mass of the particles. The initial condition for the differential equation is $\eta_\ell^{cd}(k, 0) = 0$ The phase shifts depend only on the wave number k defined by: $\eta_\ell^{cd}(k) = \lim_{r\to\infty}\eta_\ell^{cd}(k, r)$. The equation (4.10) was obtained first by Calogero [F.C67], the wave expansion method was described more detailed in Ref.[Bab76]. The method has some advantages, for instance the phase shifts has direct link with the interaction potential. It gives a possibility to look on the effect of the interaction to phase shifts behaviour. On the other hand the equation (4.10) is technically easier to solve than the Schrödinger equation.

Note that the phase function equation does not depend on the amplitude function $A_\ell^{cd}(r)$. So, calculation of the scattering phase at this potential is reduced to solving the problem with initial condition, i.e. to the Cauchy problem for the first order non-linear differential equation. Using this method the phase shifts of electron-atom scattering are calculated.

4.2 WKB-approximation

The second method is the well known WKB approximation, which is often used for calculation of the phase shifts. In this approximation the phase shifts has the form [LL88]:

$$\eta_l^{cd}(k) = \int_{r_0}^{r_c} \left[k^2 - U(r) - \frac{(l+1/2)^2}{r^2} \right]^{1/2} dr - \int_{r_1}^{r_c} \left[k^2 - \frac{(l+1/2)^2}{r^2} \right]^{1/2} dr, \qquad (4.11)$$

where r_0 is the root of $k^2 - U(r) - \frac{(l+1/2)^2}{r^2} = 0$ and $r_1 = \frac{l+1/2}{k}$. The first term of eq. (5.5) corresponds to the scattering of the particles on the central symmetrical field of the potential $U(r)$ and the second term to the free motion of the particles.

4.3 Experimental phase shifts data

Using the potentials (3.1) and (3.4), the Calogero equation (4.10) is solved. The s-wave scattering phase-shifts obtained in this way are plotted as a function of the wavenumber k in Fig. 4.3. We compare our calculations to the experimentally validated data by Schwartz *et al.*, employing different choices for the cutoff parameter r_0 in the case of the Buckingham potential, and r_D and λ_e for the RDO potential.

At $k = 0$, the singlet phase-shifts from [Sch61] tend to $\eta_0 = \pi$, corresponding to one bound state as follows from the classical Levinson theorem [Lev49], $\eta(0) = n\pi$ (n is number of bound states). The polarization potential method gives a bound state if the screening parameters that reproduce the correct H^- binding energy are applied (red dashed curve for Buckingham potential, $r_0 = 1.033\, a_B$ and blue dashed curve for RDO potential, $r_D = 4.84\, a_B$ and $\lambda_e = 0.62\, a_B$). Taking the original screening parameters in both models, we find vanishing phase-shifts at $k = 0$, i.e. no bound state. The solid line and dash-dotted line correspond to phase-shifts for rank-two and rank-one separable potential, respectively. The phase-shifts from the rank-two separable potential fully coincide with the experiments, whereas the results for the rank-one separable potential deviate at high values of k (respectively E).

We consider the s-wave scattering phase-shifts in the triplet channel in Fig. 4.3. At zero-energy the phase-shift starts off at π. Having in mind that the effective interaction between the electron and atom in the triplet channel is repulsive, this behavior obviously contradicts Levinson's theorem that predicts the scattering phase-shift to increase by π with every occurring bound state. To resolve this inconsistency, the classical Levinson theorem for one-body problems has been generalized for the scattering on a compound target by
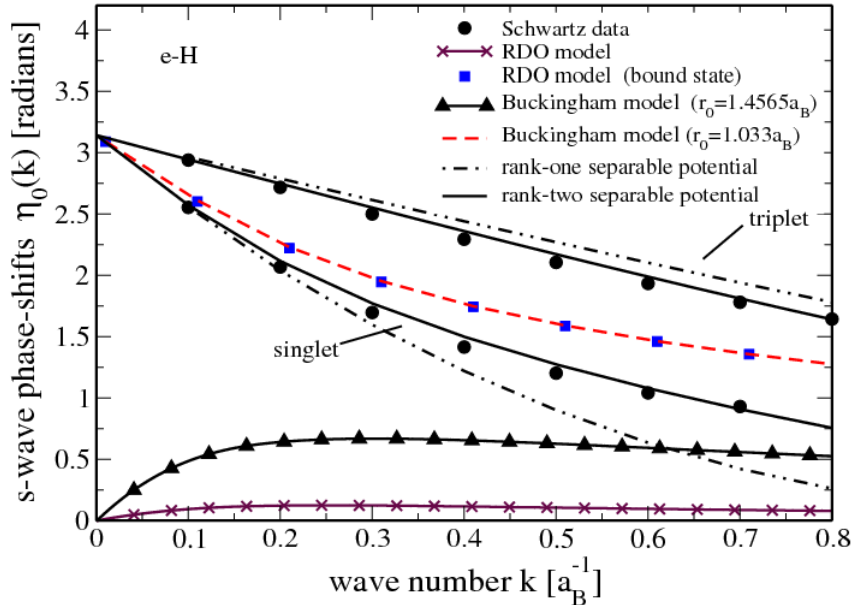
Figure 4.3: Electron-atom (e-H) scattering phase-shifts as a function of wave number k for $\ell = 0$. Shown are experimental data of Schwartz [Sch61] for the singlet and triplet channels, model calculations using the Buckingham [Eq.(3.1)] and the RDO pseudopotential [Eq.(3.4)] at different parameters, as well as different separable potentials.

Rosenberg and Spruch [RS96a]. The generalized Levinson theorem states that the phase-shift at vanishing energy is $\eta(0) = (n_{\mathrm{Pauli}} + n)\pi$, where n_{Pauli} is the number of states from which the particle is excluded by the Pauli principle. n_{Pauli} is defined by the number of nodes in the one-particle wave function. Application of the generalized Levinson theorem to the electron-hydrogen triplet scattering shows the one-particle wave function has one node, that means the zero-energy triplet phase shift is a nonzero multiple of π [RS96b]. Since the triplet electron-hydrogen wave function is spatially antisymmetric, the equivalent one-body wave function is orthogonal to the hydrogenic ground-state function and must have at least one node. Thus, our result for the behavior at zero-energy of the triplet phase-shift does not predict a triplet bound state H^-. This agrees with previous investigations of scattering of electrons on hydrogen atoms at low energies, where the scattering length was defined under the assumption that the negative hydrogen ion H^- can be formed only in the singlet channel [OO60, Gel73, RSO60, ORS62, ORS61]. In our calculations of the second virial coefficient we consider only the singlet bound state of H^-. Figs. 4.4 and 4.5 show the calculated phase-shifts for p and d waves, respectively. For comparison, the data from variational calculations [RP75] are also presented. The phase-shift is zero (no bound states) at the origin and increases monotonically. The phase-shifts for $\ell = 1$ and
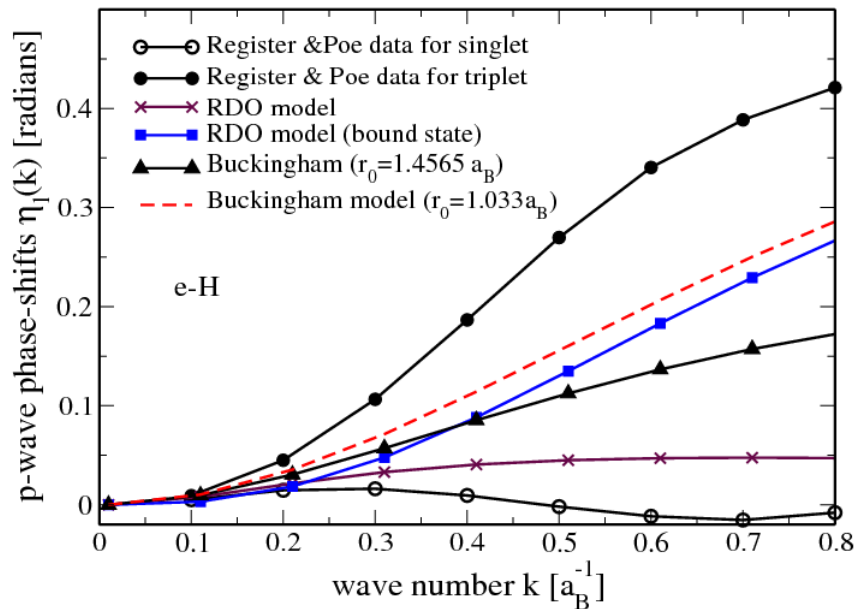
Figure 4.4: Electron-atom (e-H) scattering phase-shifts as a function of wave number k for $\ell = 1$.

$\ell = 2$ are very small in comparison to the s-wave data for the low-energy range. In general, terms from higher orbital moments are negligible for low-energies. Hence, we only apply phase-shift data for $\ell = 0, 1, 2$ in further calculations. The experimental phase shifts data, which are used for calculation of the second virial coefficients, are given in Tab. 4.1.
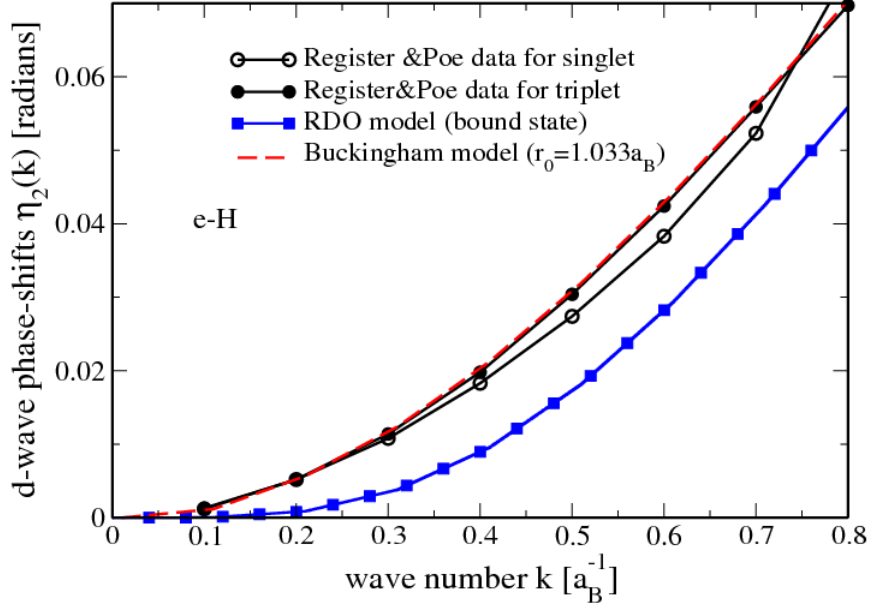
Figure 4.5: Electron-atom (e-H) scattering phase-shifts as a function of wave number k for $\ell = 2$.

Table 4.1: The experimantal phase shifts of electron scattering on hydrogen atom for $\ell = 0, 1, 2$. The phase shifts are given in radians.

k, $[a_B^{-1}]$	$\eta_0^{ea}(k)$ Ref. [Sch61]		$\eta_1^{ea}(k)$ Ref. [RP75]		$\eta_2^{ea}(k)$ Ref. [RP75]	
	singlet	triplet	singlet	triplet	singlet	triplet
0.1	2.553	2.9388	0.0051	0.0092	0.0012	0.0013
0.2	2.0673	2.7171	0.0146	0.0449	0.0052	0.0052
0.3	1.6964	2.4996	0.0162	0.1064	0.0108	0.0114
0.4	1.4146	2.2938	0.0094	0.1866	0.0183	0.0198
0.5	1.202	2.1046	-0.0019	0.2697	0.0274	0.0304
0.6	1.041	1.9329	-0.0116	0.3404	0.0383	0.0424
0.7	0.93	1.7797	-0.0154	0.3885	0.0523	0.0559
0.8	0.886	1.643	-0.008	0.4210	0.0745	0.0697

4.4   Results for total and partial cross sections

The starting point for the description of electron scattering at atom in quantum mechanics is the Schrödinger equation. Numerous methods were developed to obtain scattering cross sections. Most of the calculations were made using the close-coupling method introduced by Massey and Mohr [HM32]. In the work [PT66], the close-coupling method was used to describe elastic and inelastic collisions below ionization threshold including additional ground states in the close-coupling decomposition. The close-coupling method is capable of not only description of elastic scattering, but it is also valuable at description of inelastic processes such as excitation, ionization, capture, and resonances in [LJR08, M.A83, IS92]. Based on the R-matrix method used by Burke at all in [PCM87], integral scattering sections were calculated for electron collisions with hydrogen at moderate energies. The hybrid theory of elastic electron scattering on hydrogen which employs a combination of polarized orbits' method and optical potential formalism has been proposed in [Bha07]. This work presents calculated scattering phase shifts taking into account correlations at small and large scattering at the same time. Recent work [MWE⁺07] was devoted to studies of electron-atom scattering using time-dependent density functional calculation made it possible to obtain phase shifts for elastic electron scattering at hydrogen atom using the Cohen potential.

Partial and total elastic cross sections [LL88] for plasma particles are related to phase shifts $\eta_\ell^{cd}(k)$ according to

$$Q_\ell^{cd}(k) = \frac{4\pi}{k^2}(2\ell+1)\sin^2\eta_\ell^{cd}(k), \qquad Q^{cd}(k) = \frac{4\pi}{k^2}\sum_\ell (2\ell+1)\sin^2\eta_\ell^{cd}(k). \qquad (4.12)$$

The polarization pseudopotential model (3.4) was employed in this chapter as an interaction potential between electrons and atoms. One should remember that this pseudopotential takes into account collective and quantum-mechanical effects that are to be considered as description of elementary processes.

The phase shifts $\eta_\ell^{ea}(k,r)$ are calculated by solving the Calogero equation (4.10) for the electron scattering on atomic hydrogen. Using the obtained phase shifts the total and partial cross sections can be obtained. Fig.4.6 presents the total and partial cross sections for different values of the orbital moment ℓ, $\Gamma = 0.5$ and $r_S = 10$. One can see from the figure, the total and s-wave cross sections are essential at low energies. The partial cross sections for higher orbital moments go up with increasing of energy.

Figure 4.7 represents the comparison of total section for scattering of electron at hydrogen atom calculated within the present work and available experimental data. The experimentally treatment of the scattering on the hydrogen atom is complicated because of difficulties associated with the handling of atomic hydrogen. Therefore there are few work, which performed such experiments [BF58, Eis69, NMRT61]. Some theoretical study of collision process for electron on atom is thoroughly considered in [Tem62, OO60].

Quantum effect on elastic scattering of electron at atom is also of interest. Therefore, we studied total scattering sections as a function of de Broglie wave Λ_e, in the potential (3.4).
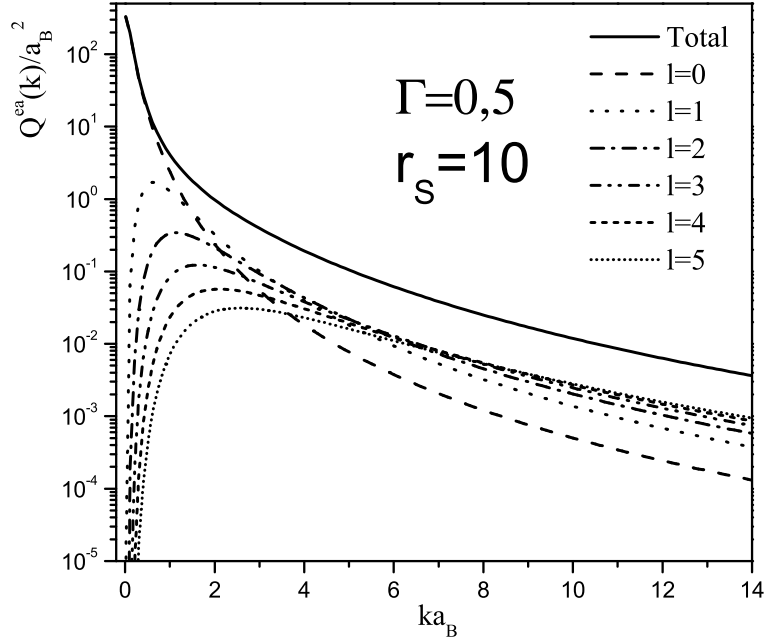
Figure 4.6: Total and partial cross sections of electrons on hydrogen atoms vs. wave number. $\Gamma = 0.5$, $r_S = 10$.

Figure 4.8 shows total electron scattering sections at hydrogen atom for ($\Lambda_e = 0.8; 1; 1.2$) and $r_D = 20$ in the units of the first Bohr radius r_B. These sections were obtained for the energies $E > 10\mathrm{Ry}(= me^4/2\hbar^2 \approx 13.6$ eV), in order to compare them with those obtained in [WSY07], where the authors also studied elastic scattering using the polarizing potential (3.4), with eikonal method applicable at $E > 9$ Ry. As one can see from Figure 4.8, at larger de Broglie waves the cross section decreases. This can be explained by lower potential at shorter distances, i.e. shorter actual radius of the potential and scattering section, when quantum effects are taken into account.

Differential cross sections are defined as:

$$\frac{d\sigma(\theta, k)}{d\Omega} = \left| \frac{1}{2ik} \sum_{\ell} (2\ell + 1)[\exp(2i\eta_{\ell}^{cd}(k)) - 1]P_{\ell}(\cos\theta) \right|^2, \tag{4.13}$$

where $P_{\ell}(\cos\theta)$ are the Legendre polynomials.

The differential cross section for scattering of electron at hydrogen atom is presented at Fig. 4.9. At small scattering angles there is a good agreement with experiment, but there is considerable discrepancy at large angles stipulated by non-consideration of spin interaction between incident and bound electrons.
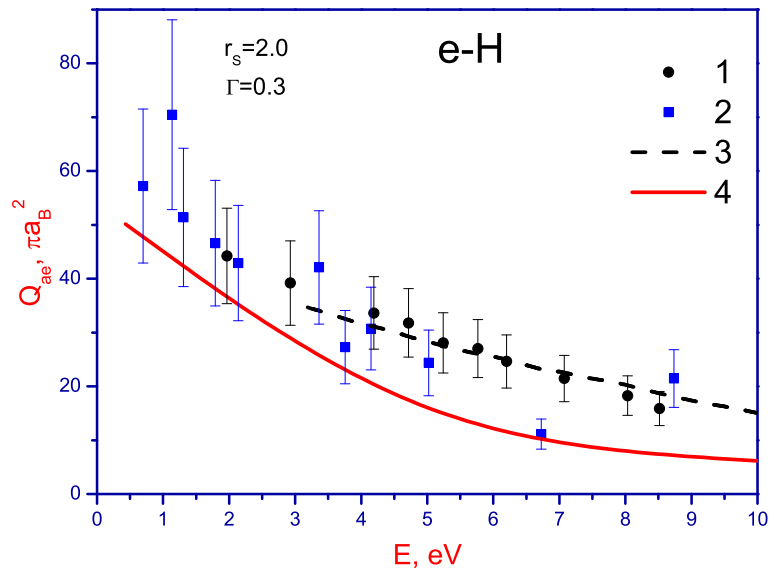
Figure 4.7: Total section for scattering of electron on hydrogen atom; 1- [BF58], 2- [Eis69], 3- [NMRT61], 4 - data of present work

Obviously, in these experimental works collision between particles are occured without plasma environment. Therefore, the theoretical curves in figures are obtained at large r_D, which correspond to small values of Γ.

Figure 4.8: Total section for scattering of electron on hydrogen atom; 1, 2, 3 - data of present work, 4,5,6 - [WSY07]
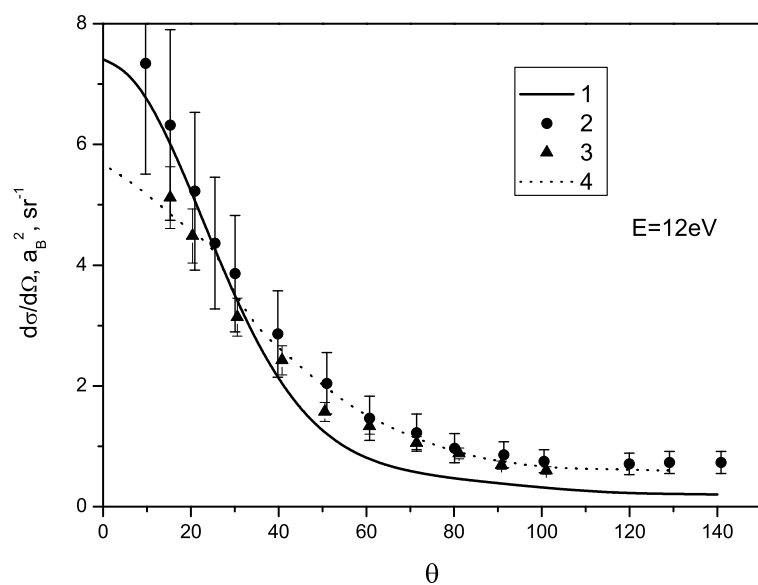
Figure 4.9: Differential sections for scattering of electron on hydrogen atom; 1 - data of present work, 2- [WC75], 3- [TLW74], 4- [BSW67]

Chapter 5

Virial expansion

5.1   Outline of virial expansion

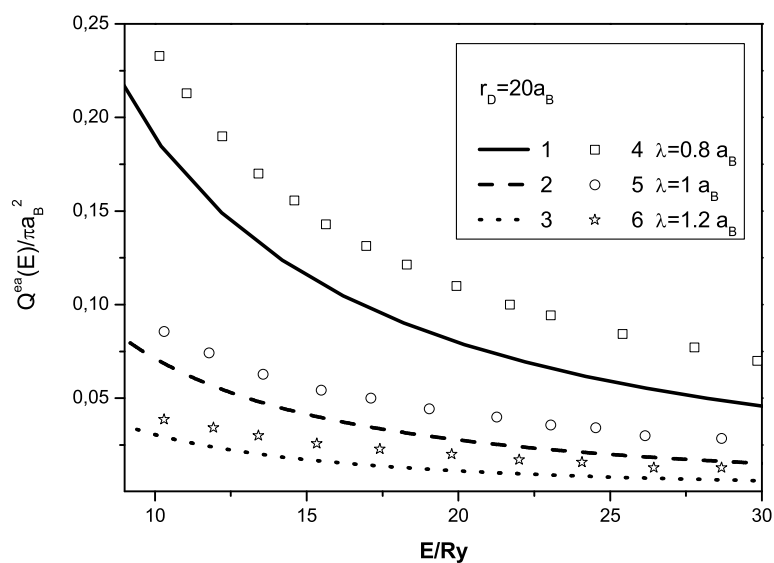A rigorous result for systems with short-range interaction is the Beth-Uhlenbeck formula that expresses the second virial coefficient in terms of the scattering phase-shifts and the bound state energies [BU37]. Some generalizations have been performed to obtain results for a larger range of densities by including medium effects, see [WDWG86, ZKK$^+$78] for charged particle systems or [SRS90] for nuclear systems. Another particularly successful method to investigate strongly correlated many-particle systems is the cluster-virial expansion [HS06]. In addition to the elementary constituents, the different bound states (cluster) are considered as new reacting species in thermal equilibrium. The thermodynamic properties are expanded in terms of the fugacities of the various components of the system and cluster-virial coefficients are introduced. In the case of nuclear systems [HS06, RSM82, TRK$^+$10], one can consider the nucleons, deuterons (two-body cluster), and alpha-particles (four-body cluster) as well as possible further nuclei as the components of the system. For ionic plasmas, electrons, ions, atoms, and molecules are such components. Another example is the electron-hole exciton system [KKK75, Zim88].

We consider the cluster-virial expansion for a partially ionized hydrogen plasma, which consists of three components as electrons (e), ions (i), and hydrogen atoms (a). The formation of heavier clusters, such as molecules or molecular ions, can also be included but this is not considered in the present work. Restricting ourselves to these three components, the relevant interactions are the elementary Coulomb interaction ($e-i$, $e-e$, $i-i$) and the more complex interaction ($e-a$, $i-a$, $a-a$) with the atoms. The Coulombic contributions to the EOS have been investigated extensively elsewhere, see Ref. [WDWG86], and will not be given here.

To keep the work as focused as possible, we consider only the electron-atom interaction, i.e. electron-atom scattering states as well as bound states, and work out its contribution to the EOS. The treatment of electron-atom interaction in EOS studies is still an open question. A widely used method consists in constructing an effective electron-atom potential. The pseudopotential method allows to include medium effects and thereby to enlarge

the region of applicability of the cluster-virial expansion. The disadvantage of the pseudopotential method is that it depends on a local, energy-independent potential that can be introduced only in certain approximations, to replace the energy dependent three-particle T-matrix. Other semiempirical methods, such as the excluded volume concept [EFF$^+$91] discussed below, depend on free parameters that lack a proper quantum-statistical foundation.

In this work, we overcome the shortcomings of the pseudopotential method by deriving results for the electron-atom virial coefficient that are based on experimental data for the electron-atom scattering cross-sections. Therefore, our results may be considered as benchmarks for the electron-atom contribution to the EOS, only limited by the accuracy of measured scattering data. We compare our results to different pseudopotential calculations. As an example, we use reconstructed separable potential for the electron-atom interaction, and consider medium effects such as self-energy and Pauli blocking.

5.2   Cluster virial expansion

5.2.1   Density expansion for the EOS

The canonical partition function of an interacting many-particle system at temperature T, volume V, composed of N_c particles per species c ($c = e$, i, a) carrying spin s_c, reads

$$Z^{\text{can}}(T, V, N_c) = \text{Tr}\left\{\exp(-\beta H)\right\}, \tag{5.1}$$

with $\beta = 1/k_{\text{B}}T$. Here and in the following, the spin of particles of species c is implicitly taken as $s_e = 1/2$ for electrons, $s_i = 1/2$ for protons and for atoms in the singlet state (antiparallel spins of electron and proton) $s_{a,\text{singlet}} = 0$, and $s_{a,\text{triplet}} = 1$ for the triplet state (parallel spins of e and i). We neglect hyperfine splitting of the atomic levels.

The Hamiltonian

$$H = \sum_c \sum_{j=1}^{N_c} \left[E_c^{(0)} + \frac{p_j^2}{2m_c}\right] + \frac{1}{2}\sum_{cd}\sum_{j=1}^{N_c}\sum_{k=1}^{N_d}{}' V_{cd}(\vec{r}_j - \vec{r}_k) \tag{5.2}$$

contains, besides the kinetic energy of each particle, the mutual interaction, represented by the two-particle interaction potential $V_{cd}(\vec{r}_j - \vec{r}_k)$. The prime indicates that self-interaction is excluded, and the energies for each component are gauged to $E_c^{(0)}$ if the particles are at rest. From a relativistic approach, $E_c^{(0)}$ is given by the rest mass containing the binding energy. In our nonrelativistic approach, we choose the gauge relatively to the rest mass of the elementary particles so that $E_c^{(0)}$ is the binding energy of the composites.

Using the Mayer cluster expansion [Hua66], we arrive at the virial expansion for the free energy $F = -k_{\text{B}}T \ln Z^{\text{can}}$ valid for short-range potentials,

$$F(T, V, N_c) = F_{\text{id}}(T, V, N_c) - k_{\text{B}}TV\left\{\sum_{cd} n_c n_d b_{cd} + \sum_{cde} n_c n_d n_e b_{cde} + ...\right\}. \tag{5.3}$$

$F_{\rm id}(T, V, N_c) = k_{\rm B}T \sum_c N_c \left[\ln\left(\frac{\Lambda_c^3 N_c}{V g_c}\right) - 1 + \beta E_c^{(0)} \right]$ is the free energy for the classical ideal (i.e. non-interacting) system, where $\Lambda_c = (2\pi\hbar^2/k_{\rm B}Tm_c)^{1/2}$ denotes the thermal wavelength of species c, and $n_c = N_c/V$ the particle number density of the component c, $g_c = 2s_c + 1$ is the spin degeneracy factor. The expansion coefficients b_{cd} and b_{cde} are the second and third virial coefficients, respectively. They are determined by the interaction, but also by degeneracy terms.

Having the virial coefficients at our disposal, we can easily derive the thermodynamic properties of the system under consideration. E.g. for the pressure and the chemical potential the following expressions are found using the standard thermodynamic relations:

$$p(T, V, N_c) = p_{\rm id}(T, V, N_c) - k_{\rm B}T\left\{ \sum_{cd} n_c n_d b_{cd} + 2 \sum_{cde} n_c n_d n_e b_{cde} + ... \right\}, \qquad (5.4)$$

$$\mu_c(T, V, N_c) = \mu_{c,\rm id}(T, V, N_c) - k_{\rm B}T\left\{ 2 \sum_d n_d b_{cd} + 3 \sum_{de} n_d n_e b_{cde} + ... \right\}, \qquad (5.5)$$

where $p_{\rm id}(T, V, N_c) = k_B T \sum_c \frac{N_c}{V}$ and $\mu_{c,\rm id}(T, V, N_c) = k_B T \ln\left(\frac{\Lambda_c^3 N_c}{V g_c}\right) + E_c^{(0)}$ are the ideal parts of the pressure and the chemical potential, respectively (for the hydrogen atom the degeneracy factor is $g_a = 4$). Note that in relativistic approaches the chemical potentials are gauged including the rest mass of the constituents, as discussed for the Hamiltonian (6.1).

Chemical equilibrium for a reaction $\nu_a A + \nu_b B \leftrightharpoons \nu_c C$ between the components A, B, C gives the relation $\nu_a \mu_a + \nu_b \mu_b = \nu_c \mu_c$. This way, the thermodynamic potentials finally depend only on the total densities of the constituents, or their chemical potentials, since the total number of the constituent particles is conserved. The densities of the composites or their chemical potentials can be eliminated, using a mass action law or a Saha equation.

Note that it is possible to derive the cluster virial expansion in a systematic way, starting from a quantum statistical approach [RSM82]. The spectral function of the elementary particle propagators is related to the self-energy. Within a cluster decomposition of the self-energy, the contribution of the different clusters can be identified considering partial sums of ladder diagrams. The first-principle approach gives a consistent introduction of the chemical picture avoiding double countings, and allows for systematic improvements.

Coming back to the partially ionized plasma, the virial expansion is diverging for the long-range Coulomb interaction. This refers to the $e - e$, $e - i$, $i - i$ contributions. Partial summations lead to convergent results, and the expansion of the thermodynamic potentials contains also terms with $n_c^{1/2}$ and $\log n_c$, see [WDWG86]. The contribution of the scattering and bound parts of the second virial coeffient for atom-atom interaction was calculated in Ref. [SK82]. In this work, we evaluate the second virial coefficient Eq. (5.20) for the electron-atom interaction.

5.2.2 Fugasity expansion for the EOS

Our starting point is the cluster virial expansion for the grand canonical partition function $\Omega(z_e, z_i, z_a, T, V)$ is a function of the fugacities

$$z_c = e^{\beta(\mu_c - E_c^{(0)})}, \tag{5.6}$$

the temperature T, and the system's volume V. For convenience, we will use the shorthand notation $\Omega(z_c, T, V)$ in the following, having in mind that z_c represents the triple of fugacities of each component. Also, we consider only terms up to the second order in the fugacities:

$$\Omega(z_c, T, V) = 1 + \sum_{c=e,i,a} z_c \Omega_c(T, V) + \sum_{c,d} z_c z_d \Omega_{cd}(T, V) + \mathcal{O}(z_c^3) . \tag{5.7}$$

Here, we have introduced the single-particle partition functions $\Omega_c(T, V) = g_c V / \Lambda_c^3$ and the two-particle partition functions $\Omega_{cd}(T, V)$, which are related to the interaction hamiltonian; $\Lambda_c = (2\pi\hbar^2/m_c k_B T)^{1/2}$ is the thermal wavelength of species c. The two-particle partition will be related to the second virial coefficient, below. From the partition function, we can directly derive the pressure P in the system,

$$P(z_c, T, V) = \frac{k_B T}{V} \ln \Omega(z_c, T, V) . \tag{5.8}$$

Replacing the partition function by Eq. (5.7) applying the expansion $\ln(1+x) = x - x^2/2 + \ldots$, and retaining again only terms in z_c^2, we arrive at

$$\begin{aligned}
\frac{P(z_c, T, V)}{k_B T} &= \sum_c \frac{g_c}{\Lambda_c^3} z_c + \sum_{cd} z_c z_d \frac{1}{V}\left(\Omega_{cd} - \frac{1}{2}\Omega_c\Omega_d\right) + \mathcal{O}(z_c^3) \\
&= \frac{2z_e}{\Lambda_e^3} + \frac{2z_i}{\Lambda_i^3} + \frac{z_a}{\Lambda_a^3} + z_e^2\frac{\Omega_{ee} - \frac{1}{2}\Omega_e^2}{V} + z_i^2\frac{\Omega_{ii} - \frac{1}{2}\Omega_i^2}{V} + z_a^2\frac{\Omega_{aa} - \frac{1}{2}\Omega_a^2}{V} \\
&\quad + 2z_e z_i \frac{\Omega_{ei} - \frac{1}{2}\Omega_e\Omega_i}{V} + 2z_e z_a \frac{\Omega_{ea} - \frac{1}{2}\Omega_e\Omega_a}{V} + 2z_i z_a \frac{\Omega_{ia} - \frac{1}{2}\Omega_i\Omega_a}{V} + \mathcal{O}(z_c^3) . \quad (5.9)
\end{aligned}$$

The second virial coefficients are defined as $\tilde{b}_{cd} = \frac{\Lambda_c^3}{g_c}(\Omega_{cd} - \frac{1}{2}\Omega_c\Omega_d)/V$ that are related to the symmetric expressions $b_{cd} = \frac{\Lambda_d^3}{g_d}\tilde{b}_{cd}$:

$$\tilde{b}_{ee} = \frac{\Lambda_e^3}{g_e V}\left(\Omega_{ee} - \frac{1}{2}\Omega_e^2\right) \qquad \tilde{b}_{ii} = \frac{\Lambda_i^3}{g_i V}\left(\Omega_{ii} - \frac{1}{2}\Omega_i^2\right) \qquad \tilde{b}_{aa} = \frac{\Lambda_a^3}{g_a V}\left(\Omega_{aa} - \frac{1}{2}\Omega_a^2\right)$$

$$\tag{5.10}$$

$$\tilde{b}_{ei} = \frac{\Lambda_e^3}{g_e V}\left(\Omega_{ei} - \frac{1}{2}\Omega_e\Omega_i\right) \quad \tilde{b}_{ea} = \frac{\Lambda_e^3}{g_e V}\left(\Omega_{ea} - \frac{1}{2}\Omega_e\Omega_a\right) \quad \tilde{b}_{ia} = \frac{\Lambda_i^3}{g_i V}\left(\Omega_{ia} - \frac{1}{2}\Omega_i\Omega_a\right) ,$$

which allows us to rewrite Eq. (5.9) as

$$
\frac{P(z_c, T, V)}{k_B T} = \sum_c \frac{g_c}{\Lambda_c^3} \left(z_c + \sum_d z_c z_d \tilde{b}_{cd} \right) .
\tag{5.11}
$$

The thermodynamic functions of the partially ionized hydrogen plasma are derived from the grand canonical potential Eq. (5.7). First, we evaluate the number densities of each component,

$$
n_c = z_c \left(\frac{\partial}{\partial z_c} \frac{\ln \Omega(z_c, T, V)}{V} \right)_{T,V} = z_c \left(\frac{\partial}{\partial z_c} \frac{P(z_c, T, V)}{k_B T} \right)_{T,V}
$$
$$
= \frac{g_c}{\Lambda_c^3} \left(z_c + 2 \sum_d z_c z_d \tilde{b}_{cd} + \mathcal{O}(z_c^3) \right) .
\tag{5.12}
$$

In terms of the second virial coefficient, evaluation of the derivatives with respect to the fugacity yields

$$
n_e = \frac{g_e}{\Lambda_e^3} \left(z_e + 2 z_e^2 \tilde{b}_e + 2 z_e z_i \tilde{b}_{ei} + 2 z_e z_a \tilde{b}_{ea} \right) ,
\tag{5.13}
$$
$$
n_i = \frac{g_i}{\Lambda_i^3} \left(z_e + 2 z_i^2 \tilde{b}_i + 2 z_i z_e \tilde{b}_{ei} + 2 z_i z_a \tilde{b}_{ia} \right) ,
\tag{5.14}
$$
$$
n_a = \frac{g_a}{\Lambda_a^3} \left(z_a + 2 z_a^2 \tilde{b}_a + 2 z_a z_i \tilde{b}_{ia} + 2 z_a z_e \tilde{b}_{ea} \right) .
\tag{5.15}
$$

In the first terms of equations (5.13), (5.14), and (5.15), respectively, we recognize the partial densities of the ideal (non-interacting) system, $n_{c,\text{id}} = (g_c) z_c / \Lambda_c^3$. Next, we evaluate the entropy density of the partially ionized plasma (z_c is a function of μ_c and T),

$$
\frac{S(z_c, T, V)}{V} = \left(\frac{\partial P(z_c, T, V)}{\partial T} \right)_{z_c, V} = \frac{\partial}{\partial T} \left(k_B T \frac{\ln \Omega(z_c, T, V)}{V} \right)_{z_c, V}
$$
$$
= \frac{P(z_c, T, V)}{T} + \frac{k_B T}{V} \left(\frac{\partial \ln \Omega(z_c, T, V)}{\partial T} \right) .
\tag{5.16}
$$

Substituting the Eq.(5.11) in (5.16) and using (5.6) we obtain

$$
\begin{aligned}
\left(\frac{\partial P(z_c, T, V)}{\partial T}\right)_{\mu_c} &= \frac{\partial}{\partial T} \sum_c g_c \left(\frac{m_c k_B}{2\pi\hbar^2}\right)^{3/2} k_B T^{5/2} \left[e^{\frac{1}{k_B T}\left(\mu_c - E_c^{(0)}\right)}\right. \\
&+ \left. \sum_d e^{\frac{1}{k_B T}\left(\mu_c - E_c^{(0)}\right)} e^{\frac{1}{k_B T}\left(\mu_d - E_d^{(0)}\right)} \tilde{b}_{cd}(T, V)\right] \\
&= \frac{5}{2}\frac{P}{T} + \sum_c \frac{g_c}{\Lambda_c^3} k_B T \left[e^{\frac{1}{k_B T}\left(\mu_c - E_c^{(0)}\right)}\left(-\frac{1}{T}\right)\ln z_c\right. \\
&+ \left. \sum_d e^{\frac{1}{k_B T}\left(\mu_c - E_c^{(0)} + \mu_d - E_d^{(0)}\right)}\left(-\frac{1}{T}\right)\left[\ln z_c + \ln z_d\right]\tilde{b}_{cd}(T, V)\right] \\
&+ \sum_{cd} \frac{g_c}{\Lambda_c^3} k_B T z_c z_d \frac{\partial}{\partial T}\tilde{b}_{cd}(T, V) \\
&= \frac{5}{2}\frac{P}{T} - k_B \sum_c n_c \ln z_c + k_B T \sum_{cd} \frac{g_c z_c z_d}{\Lambda_c^3}\frac{\partial \tilde{b}_{cd}(T)}{\partial T} \qquad (5.17)
\end{aligned}
$$

The density of internal energy follows from the relation

$$
\frac{U(z_c, T, V)}{V} = \frac{TS}{V} + \sum_c \mu_c n_c - P = \frac{3}{2}P - \sum_c n_c E_c
$$
$$
+ k_B T^2 \sum_{cd} \frac{g_c z_c z_d}{\Lambda_c^3}\frac{\partial \tilde{b}_{cd}}{\partial T} \qquad (5.18)
$$

And finally, we find for the free energy density $f(n_c, T) = F/V$ after eliminating z_c with Eq.(5.13)

$$
\begin{aligned}
f(n_c, T) &= \frac{U}{V} - \frac{TS}{V} = \sum_c \mu_c n_c - P \\
&= k_B T \sum_c n_c \left[\ln\frac{\Lambda_c^3 n_c}{g_c} - 1 + \beta E_c^{(0)}\right] \\
&- k_B T \sum_{cd} n_c n_d b_{cd} \qquad (5.19)
\end{aligned}
$$

that coincides with the expression (5.3).

5.2.3 The Beth-Uhlenbeck formula

In this paper we are concerned with the evaluation of the second virial coefficient that describes the non-ideality corrections in lowest order with respect to the densities. According to Beth and Uhlenbeck [BU37, KSK05, LL88], for a central symmetric interaction potential the following formula has been derived, which relates the second virial coeffient to the

energy eigenvalues $E_{n\ell}^{cd}$ of the two-particle bound state $|n\ell\rangle$ and the scattering phase-shifts $\eta_\ell^{cd}(E)$ describing the two-particle scattering states,

$$b_{cd} = \frac{\Lambda_d^3}{g_d}\left[\delta_{cd}\tilde{b}_{cd}^{(0)} + \tilde{b}_{cd}^{\text{bound}} + \tilde{b}_{cd}^{\text{sc}}\right] , \qquad (5.20)$$

where

$$\tilde{b}_{cd}^{(0)} = \begin{cases} 2^{-5/2} & \text{(ideal Bose gas)} \\ -2^{-5/2} & \text{(ideal Fermi gas)} \end{cases} \qquad (5.21)$$

is the second virial coefficient for the ideal quantum gas.

In this work we calculate the second virial coefficient for the $e-a$ contribution. The spin degrees of freedom of the bound electron and the scattering electron give rise to a singlet (antiparallel electron spins) and a triplet (parallel electron spins) scattering state; the proton spin contributes a spin degeneracy factor $g_i = 2$. The total second virial coefficient $b_{ae} = b_{ea}$ is defined with the total density of atoms and electrons. It is decomposed into the singlet contribution and the triplet contribution, so that $b_{ae} = b_{ae}^{\text{singlet}} + b_{ae}^{\text{triplet}}$. For convenience, we introduce the dimensionless coefficient $\tilde{b}$ that appears in the fugacity expansion as $\tilde{b}_{ea} = \frac{g_a}{\Lambda_a^3}b_{ea}$, $\tilde{b}_{ae} = \frac{g_e}{\Lambda_e^3}b_{ae}$. Note that $\tilde{b}_{ea}$ is no longer symmetric with respect to a change of indices, instead, we find $\tilde{b}_{ea} = 2\left(\frac{m_a}{m_e}\right)^{3/2}\tilde{b}_{ae}$. Since $m_e \ll m_a$ we have $\Lambda_{ea}^3/\Lambda_a^3 \approx 1$, from which follows that the dimensionless second virial coefficient is again the sum of the corresponding dimensionless singlet and triplet coefficients, $\tilde{b}_{ae} = \tilde{b}_{ae}^{\text{singlet}} + \tilde{b}_{ae}^{\text{triplet}}$.

The bound part of the second virial coefficient for the singlet state $\tilde{b}_{ae}^{\text{bound,singlet}}$ has the following form:

$$\tilde{b}_{ae}^{\text{bound,singlet}} = \frac{1}{4}\sum_{\ell=0}^\infty (2\ell+1)\sum_{n\geq\ell+1} e^{-\beta E_{n\ell}^{ae}} , \qquad (5.22)$$

where ℓ denotes the angular momentum of the two-particle system. The scattering part of the second virial coefficient $\tilde{b}_{ae}^{\text{sc}}$ consist of the singlet and triplet parts:

$$\tilde{b}_{ae}^{\text{sc,singlet}} = \frac{1}{4}\sum_{\ell=0}^\infty (2\ell+1)\left[\frac{1}{\pi}\int_0^\infty e^{-\beta E}\frac{d}{dE}\eta_\ell^{ae,\text{singlet}}(E)\,dE\right] \qquad (5.23)$$

$$\tilde{b}_{ae}^{\text{sc,triplet}} = \frac{3}{4}\sum_{\ell=0}^\infty (2\ell+1)\left[\frac{1}{\pi}\int_0^\infty e^{-\beta E}\frac{d}{dE}\eta_\ell^{ae,\text{triplet}}(E)\,dE\right] \qquad (5.24)$$

At this point, we would like to make a short note regarding different forms of the Beth-Uhlenbeck formula Eq.(5.20) that can be found in the literature. We use formula Eq.(5.20), which has been derived originally by Beth and Uhlenbeck [BU37], see also Refs [Hua66, LL88]. After partial integration of the Eq.(5.20) one obtains another form for the Beth-Uhlenbeck formula, see e.g. [SRS90, HS06], where the scattering phase shift arises instead of its derivative, and from the integration an additional term $-\eta_\ell^{cd}(0)/\pi$ appears, which is sometimes condensed into the bound part [HS06].

Chapter 6

Results for the second virial coefficient

6.1   Atom-atom contribution

In this section we look at the atom-atom pairs. As interaction potential between H atoms for singlet state of bound electrons a hard core with square well potential is taken. The parameters for singlet state $V_0 = -4.658$ eV, the range $d = 0.944 \cdot 10^{-8}$cm, collision diameter $a = 0.503 \cdot 10^{-8}$cm, for triplet state a hard sphere potential with temperature dependent collision diameter $a(T)$ (for example at $T = 10^4 K$ $a = 1.602 \cdot 10^{-8}$cm are taken from Ref.[SK62]. In Ref.[SK62] bound and scattering phase shifts has been obtained using the Jost functions. In this work binding energy is determined from the Schrödinger equation, phase shifts are obtained by solving the Calogero equation [Bab76] and using WKB-approximation. The Beth-Uhlenbeck formula for $H - H$ second virial coefficient is [SK62]

$$b_{HH}(T) = 4\pi\sqrt{\pi}\Lambda_{HH}^3 \sum_{\ell=0}^{\infty}(2\ell+1)\left[1 - \frac{(-1)^\ell}{2s_p+1}\right]$$

$$\times \left\{\sum_n \exp(-\beta E_{n\ell}) + \frac{2\Lambda_{HH}^2}{\pi}\int_0^\infty \exp(-\Lambda_{HH}^2 k^2)k\eta_\ell^{HH}(k)dk\right\}, \tag{6.1}$$

where s_p is the spin of protons. The first term describes the bound states and the second term contains the scattering states. In the triplet channel, as was already mentioned, we use a hard sphere model and there are no bound states. In the singlet case, bound states as H_2 can appear. The formation of bound states can be observed by the localization of the wave function of the incident particle. Solving the radial Schrödinger equation:

$$u_\ell''(r) + \frac{2m}{\hbar^2}(E_{n\ell} - U_{cd}(r))u_\ell(r) - \frac{\ell(\ell+1)}{r^2}u_\ell(r) = 0 \tag{6.2}$$

we obtaine the binding energy $E_{n\ell}$ of H_2.
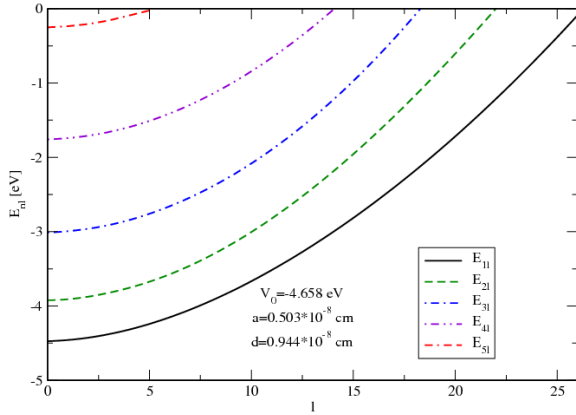
Figure 6.1: The binding energy of H_2 in dependence on the orbital moment ℓ at the $V_0 = -4.658$ eV
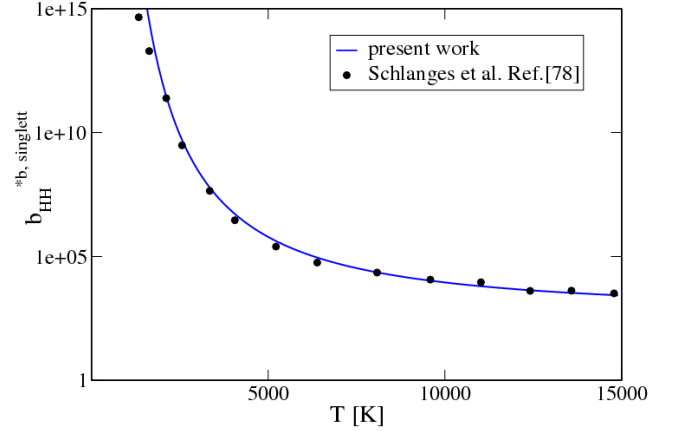
Figure 6.2: The bound state part of the second virial coefficient for singlet case of the atom-atom interaction

We have considered the $E_{n\ell}$ for different orbital momenta ℓ for $V_0 = -4.658$ eV. This dependence is presented in Fig. 6.1. As one can see, the bound states exist till $\ell = 26$.

Using Eq. (6.1) the bound state part of the second virial coefficient has been obtained, the result is presented in Fig. 6.2. We use the following convention in order to compare with results of Ref. [SK62] $b_{HH}^{*\mathrm{bound}} = (1/4)b_{HH}^{\mathrm{bound,singlet}}/4\pi\sqrt{\pi}\Lambda_{HH}^3$. The results fully coincide with the calculations of Ref. [SK62]

To obtain the scattering part of the second virial coefficient, the Calogero equation and WKB approximation are applied. Figs. 6.3 and 6.4 show the phase shifts for triplet and singlet scattering channels, respectively. In Fig. 6.3 the difference between the two methods is shown. Figure 6.4 presents the behaviour of the phase shifts in dependence of the orbital momenta ℓ. As we expected from the binding energy (Fig.4.4), the phase shifts show the presence of the bound states at different orbital moments. For example, for $\ell = 0$ till $\ell = 5$ we have 5 bound states and the last bound state appeares at $\ell = 26$.

Using the calculated phase shifts, we can obtain the second virial coefficient by formula (6.1). The maximal value of the ℓ can be estimated as: $\ell_{\max} = \mathrm{Int}(k\sigma - 1/2)$ [BU37], where $k = 2\pi/\Lambda_{HH}$. In Fig. 6.5 the triplet second virial coefficient is shown in comparison to the results obtained in Ref. [SK62]. The difference between phase shifts obtained by solving the Calogero equation and the WKB approach is also shown. The results from solving Calogero equation completely coincide with the data of Ref. [SK62]. The phase shifts in the Ref.[SK62] were calculated using the Jost functions [SK82]:

$$\eta_\ell^{cd} = \arctan\left[\frac{\Im F_\ell(k)}{\Re F_\ell(k)}\right], \tag{6.3}$$

here $F_\ell(\pm k)$ are the Jost functions.
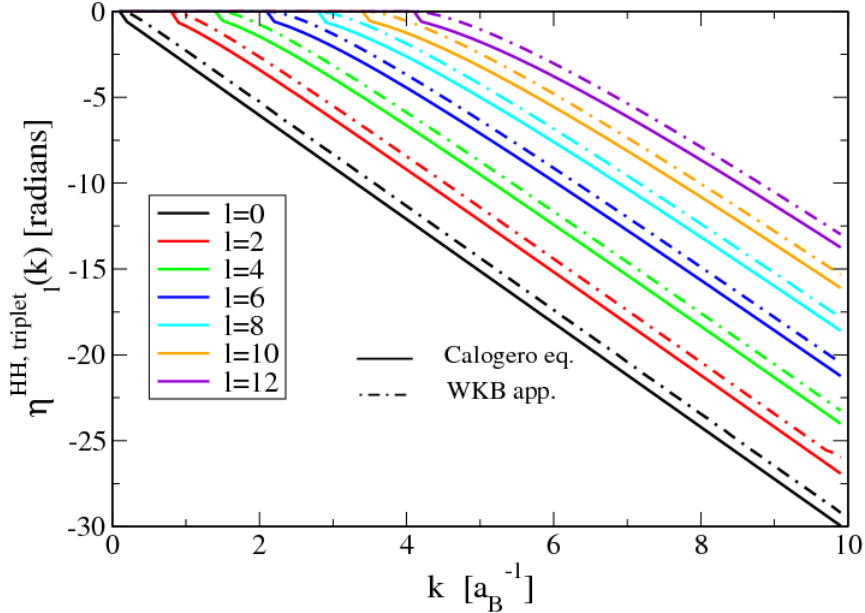
Figure 6.3: The phase shifts vs. wave number for triplet channel with two methods as the Calogero equation and the WKB approximation.

One can see from Fig. 6.5 that the contribution of the scattering part is essential at high temperatures, while the bound state part (Fig.4.5) is important at low temperature.

The good agreement of our results with the data of [SK62] shows the validity of our calculations. The next of our research is to consider the second virial coefficient for electron-atom pair with the experimental phase shifts data; to calculate the thermodynamical functions of partially ionized Hydrogen plasma.

6.2   Electron-atom contribution

The good agreement between experimental cross-sections and the variational scattering phase-shifts from Refs. [Sch61, RP75] allows us to use the latter as "experimentally confirmed" data for calculations of the second virial coefficient using the Beth-Uhlenbeck formula (5.20). The phase-shifts obtained from pseudopotential models (3.1) and (3.4) are not applied here to calculate $\tilde{b}_{ae}$.

Tabs. 6.1 and 6.2 show results for the normalized second virial coefficients $\tilde{b}_{ae}^{\text{sc,singlet}}(T)$, $\tilde{b}_{ae}^{\text{bound,singlet}}(T)$ for the singlet channel and $\tilde{b}_{ae}^{\text{sc,triplet}}(T)$ for the triplet channel, respectively. The second, third and fourth columns of both tables present data for the contribution of s, p and d waves to the scattering part of the second virial coefficient for singlet and triplet channels, respectively. Higher order contributions are small and negligible for this
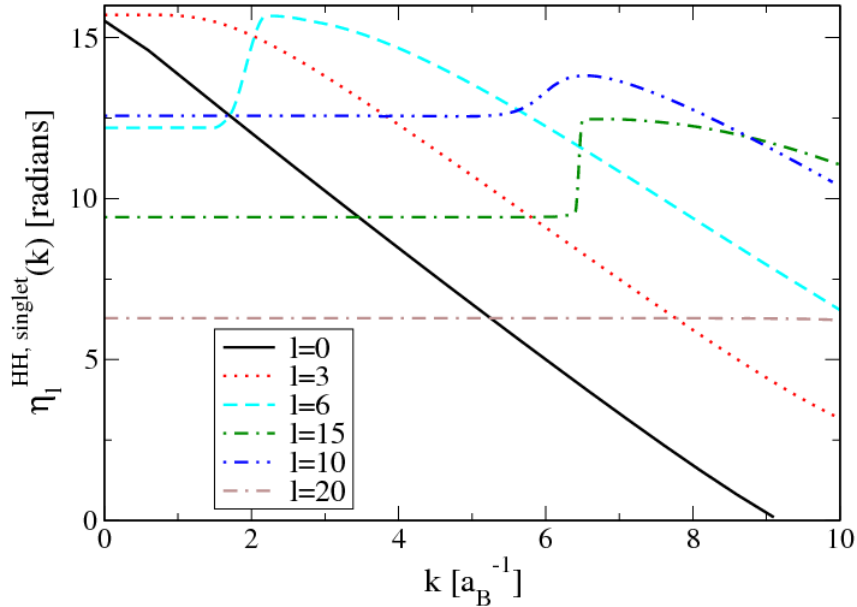
Figure 6.4: The phase shifts vs. wave number for singlet channel by solving of the Calogero equation.

temperature range. The singlet bound part of the second virial coefficient for the singlet channel is shown as the fifth column of Tab. 6.1. The binding energy is taken as $E_B^{eH} = -0.7542$ eV [MW74]. The full scattering part of the second virial coefficient is shown in the sixth column of both tables. The last column of the Tab. 6.2 presents the results for the full second virial coefficient: $\tilde{b}_{ae}(T) = \tilde{b}_{ae}^{\text{sc,singlet}}(T) + \tilde{b}_{ae}^{\text{sc,triplet}}(T) + \tilde{b}_{ae}^{\text{bound,singlet}}(T)$.

We find that the scattering contributions to the second virial coefficient increases with temperature in contrast to the bound state contribution. In Tabs. 6.1 and 6.2 the s-wave contribution to the second virial coefficient is the dominant term, p-wave and d-wave contributions are of the order of few percent.

6.3 Equation of state and thermodynamics

6.3.1 Composition

The virial expansion allows to determine a thermodynamic potential that gives all thermodynamic variables. We discussed the free energy $F(T, V, N_c)$ or the grand potential $-pV = J(T, V, \mu_c)$. Because of reactions in the system, the particle numbers of the different components are related by the chemical equilibrium conditions so that the number of independent variables is reduced. In the case of a hydrogen plasma considered here, we
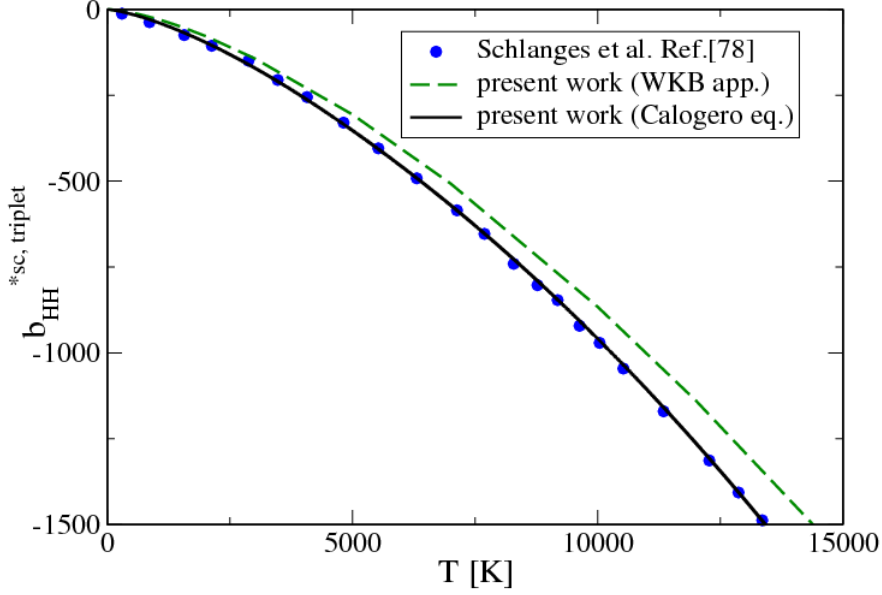
Figure 6.5:   The scattering part of the second virial coefficient for triplet case.
$b_{HH}^{*\mathrm{sc,triplet}}(T) = \frac{3}{4} b_{HH}^{\mathrm{triplet}}(T)/(4\pi\sqrt{\pi}\Lambda_{HH}^3)$.

start from the particle numbers of free electrons, free ions, and atoms, disregarding heavier
clusters. The atomic density is related to the free electron and ion density due to the Saha
equation that follows from the equilibrium condition $\mu_e + \mu_i = \mu_a$. The remaining two
particle numbers, $N_c^{\mathrm{tot}} = N_c + N_a$ with $c = e, i$, will coincide if a charge-neutral plasma
is considered so that we end up with only one particle number $N = N_e^{\mathrm{tot}} = N_i^{\mathrm{tot}}$ for a
charge-neutral hydrogen plasma in chemical equilibrium.

To derive the composition from the chemical equilibrium condition we express the
chemical potentials in terms of the densities, see Eq. (5.5). In lowest order of the cluster
virial expansion, the ideal Saha equation

$$\frac{1 - \alpha}{\alpha^2} = n_e^{\mathrm{tot}} \Lambda_e^3 \, \exp\left[\beta I^{\mathrm{eff}}(n_e, T)\right] \;, \tag{6.4}$$

is obtained for the degree of ionization $\alpha = n_e/n_e^{\mathrm{tot}}$, where $I_{\mathrm{id}}^{\mathrm{eff}}(n_e, T) = |E_a^0|$.

We will not discuss here the more general expressions where the excited states and
higher clusters are included [WDWG86]. The thermal wavelength for the atom was ap-
proximated by the thermal wavelength for the ion.

Taking the non-ideal terms into account, e.g. according to a virial expansion, the
composition follows from a Saha equation with shifted energies [KSK05]

$$I^{\mathrm{eff}}(n_e^{\mathrm{tot}}, n_i^{\mathrm{tot}}, T) = |E_a^0| - \Delta_a + \Delta_e + \Delta_i \;. \tag{6.5}$$

The energy shifts Δ_c of the different components can be obtained from density expansions. As an approximation we take the Debye shift $\Delta_e = \Delta_i = -\kappa e^2/2$ due to the Coulomb interaction between the charged particles, $\kappa = [n_e^{\mathrm{free}} e^2/\epsilon_0 \, k_\mathrm{B} T]^{1/2}$ is the inverse Debye screening length. These terms are of the order $n_e^{1/2}$. The bound energy shift Δ_a is not taken into account here because it is of higher order in density.

In Fig. 6.6 we plot the solution of the Saha equation (6.4) in dependence of the total electron density for temperatures $T = 15000\,\mathrm{K}, 20000\,\mathrm{K}$, and $30000\,\mathrm{K}$. The degree of ionization is decreasing with increasing density due to formation of bound states. The effective bound state ionization energy I^{eff} is lowering due to plasma screening. Ultimately, this leads to the Mott effect, i.e. the non-thermal ionization at high densities, due to the lowering of the ionization threshold, leads to the abrupt increase of the ionization degree, see also Refs. [WDWG86, KSK05]. We refrain from giving an exhaustive description of the Mott effect including more sophisticated analysis of the shifts and restrict ourselves only to the general behavior of the ionization degree. Note, that the virial expansion can only be applied to the low density range where the corrections are small.
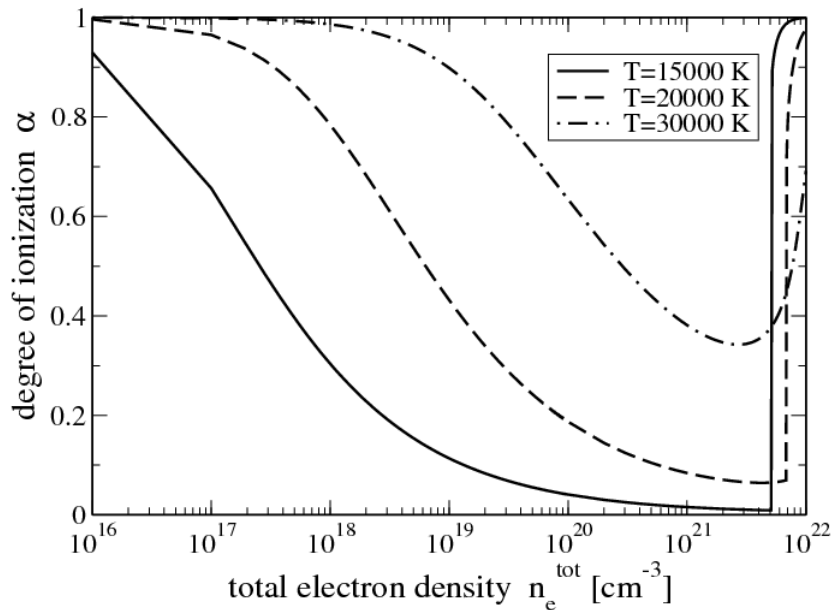
Figure 6.6: Degree of ionization as a function of the total electron density for three different temperatures, $T = 1.5, 2, 3 \cdot 10^4\,\mathrm{K}$.

6.3.2 Chemical potential, free energy, pressure

To discuss the contribution of electron-atom scattering to the chemical potential (5.5), free energy (6.2), and pressure (5.4) we rewrite the definitions as

$$\Delta\mu_{ea} = \mu^e(T, n_c) - \mu_{\text{id}}^e = -2k_B T n_a b_{ea}(T) , \tag{6.6}$$

$$\Delta F_{ea} = F(T, n_c) - F_{\text{id}} = p(T, n_c)V - p_{\text{id}}V$$
$$= -2k_B TV n_e n_a b_{ea}(T) . \tag{6.7}$$

The remaining contributions to the second virial coefficient due to the other combinations of components will not be discussed here, see [WDWG86, KSK05].

As mentioned before, the second virial coefficient can be decomposed into the singlet and triplet channel and it is given as the sum of scattering and bound state contributions,

$$b_{ea}(T) = b_{ae}(T) = \frac{\Lambda_e^3}{2}\left[\tilde{b}_{ae}^{\text{sc,singlet}}(T) + \tilde{b}_{ae}^{\text{sc,triplet}}(T)\right.$$
$$\left. + \tilde{b}_{ae}^{\text{bound,singlet}}(T)\right] . \tag{6.8}$$

The various terms are given in Tabs 6.1 and 6.2,

In Fig. 6.7, we plot the $e-$H scattering contribution to the chemical potential $\Delta\mu_{ea} = -2k_B T n_a b_{ea}(T)$ as a function of the total electron number density for $T = 10000\,\text{K}$ and $T = 15000\,\text{K}$. In a similar way, we treat the $e-$H contribution to the free energy $\Delta F_{ea} = -2k_B TV n_e n_a b_{ea}(T)$ and to the pressure $\Delta p_{ea} = -2k_B T n_e n_a b_{ea}(T)$.

6.3.3 Comparison of the results with the excluded volume concept

An alternative approach to evaluate the non-ideality term due to the neutral atoms is the excluded volume concept [EFF$^+$91]. The excluded volume is defined by the filling parameter $\eta = \frac{4}{3}\pi r_a^3 n_a$ as the volume that is occupied by atoms such that the effective volume available for the moving particles is $V^* = V(1 - \eta)$. The atom radius r_a is an empirical parameter of the order of a_{B} that has been fixed in different ways (see Ref. [EFF$^+$91]). Within the excluded volume concept, the non-ideality part of the free energy reads

$$\Delta F_{ea}^{\text{ex}} = F_{\text{id}}(T, V^*, N_e, N_i, N_a) - F_{\text{id}}(T, V, N_e, N_i, N_a)$$
$$= \frac{4}{3}\pi r_a^3 k_B T N_a[n_e + n_i + n_a]. \tag{6.9}$$

The corresponding second virial coefficient for the electron-atom pair results as

$$b_{ea}^{\text{ex}} = -\frac{2}{3}\pi r_a^3 . \tag{6.10}$$

It is instructive to note that this expression is equal to the classical second virial coefficient within the Beth-Uhlenbeck approach using a hard-sphere electron-ion potential
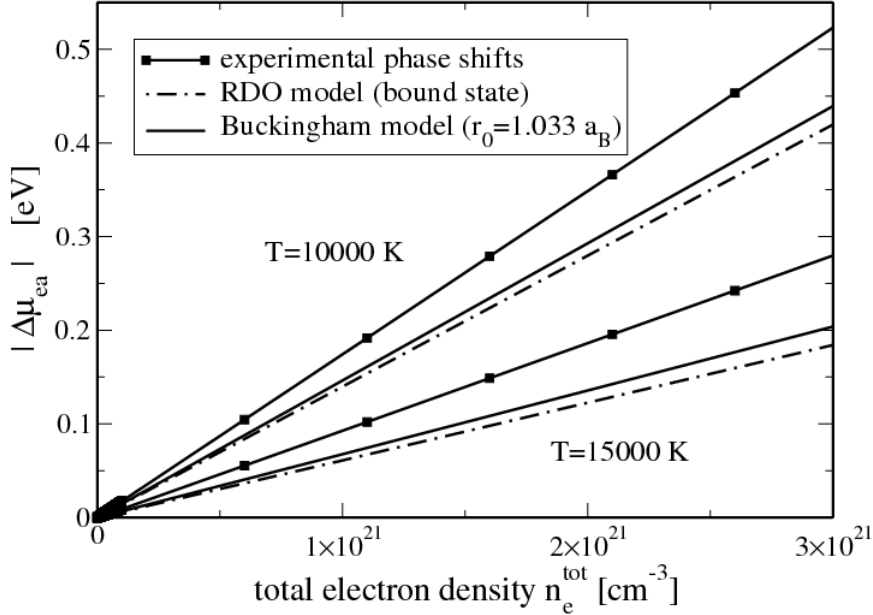
Figure 6.7: Contribution of electron–hydrogen interaction to the chemical potential as a function of the total electron density; squares represent calculations based on experimental phase-shift data, the solid line uses the Buckingham pseudopotential, the dot-dashed line uses the RDO model.

with the hard-sphere radius equal to the atom radius of the excluded volume concept r_a [EFF$^+$91]. It does not depend on the temperature of the system. For a typical atom radius of $r_a = 1.0\,a_{\mathrm{B}}$ we find $b_2^{\mathrm{class}} = b_{ea}^{\mathrm{ex}} = -3.1 \times 10^{-25} \mathrm{cm}^3$.

In Fig. 6.8 we show the second virial coefficient for the triplet state, calculated by the Beth-Uhlenbeck formula using the experimental phase-shifts from [Sch61] in comparison with the excluded volume virial coefficient for different values of r_a. In the triplet state we have a strong repulsion between electrons and atoms, hence the hard-sphere potential can be expected to give reasonable results. Because of the bound state formation, the singlet state can not be treated within the excluded volume approach. Note that in contrast to the excluded volume concept and the hard-sphere model, our results indeed depend on the temperature. At high temperatures ($T \gtrsim 50000\,\mathrm{K}$), the second virial coefficient from our Beth-Uhlenbeck calculation approaches the excluded volume virial coefficient for the atom radius $r_a = 1.2\,a_B$. In this sense, the Beth-Uhlenbeck using experimentally validated scattering phase-shifts provides a benchmark to the semi-empirical excluded volume model.

Although the excluded volume concept is widely applied to take into account the presence of atoms in the plasma, this method gives only approximate results. The dependence of the atom subsystem on the plasma parameters was included in the confined atom model [WDWG86, GHR69] due to an atomic radius. These methods cannot cover numerous ef-

fects in the electron-atom interaction, such as the spin dependence, scattering phase-shifts, and bound states which are included in the Beth-Uhlenbeck formula.
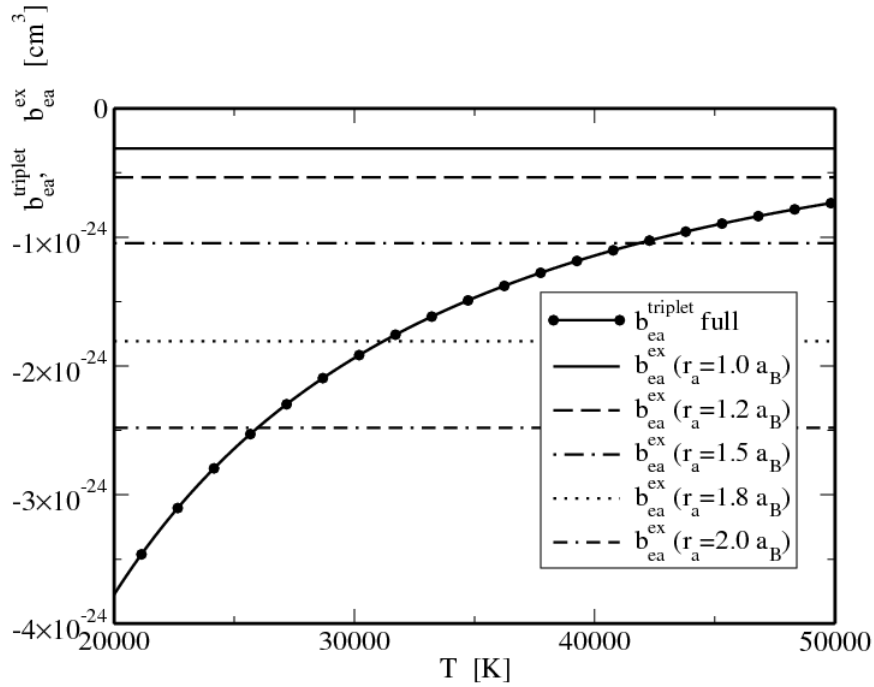
Figure 6.8: Second virial coefficient in the triplet channel as function of temperature. The Beth-Uhlenbeck result (solid line with circles) is compared to the excluded volume model for different values of r_a

Table 6.1: The singlet scattering and bound parts of the second virial coefficient for $e - H$ interaction. Contribution of different partial waves and bound state contribution are given.

T, K	$\tilde{b}_{ae}^{\text{sc,singlet}}$, s-wave	$\tilde{b}_{ae}^{\text{sc,singlet}}$, p-wave	$\tilde{b}_{ae}^{\text{sc,singlet}}$, d-wave	$\tilde{b}_{ae}^{\text{bound,singlet}}$	$\tilde{b}_{ae}^{\text{singlet}}$ full
5000	-0.0499	0.0012	0.0007	1.4401	1.3922
6000	-0.0541	0.0015	0.0008	1.0756	1.0239
7000	-0.0578	0.0017	0.0010	0.8732	0.8181
8000	-0.0611	0.0018	0.0012	0.7468	0.6887
9000	-0.0642	0.0020	0.0013	0.6613	0.6005
10000	-0.0670	0.0021	0.0015	0.6000	0.5366
11000	-0.0696	0.0022	0.0016	0.5541	0.4883
12000	-0.0720	0.0022	0.0018	0.5185	0.4505
13000	-0.0743	0.0023	0.0019	0.4902	0.4202
14000	-0.0765	0.0023	0.0021	0.4672	0.3952
15000	-0.0785	0.0024	0.0022	0.4481	0.3742
16000	-0.0805	0.0024	0.0024	0.4321	0.3564
17000	-0.0823	0.0024	0.0025	0.4184	0.3411
18000	-0.0840	0.0024	0.0026	0.4066	0.3277
19000	-0.0857	0.0024	0.0028	0.3963	0.3159
20000	-0.0873	0.0024	0.0029	0.3873	0.3054
21000	-0.0888	0.0024	0.0031	0.3793	0.2960
22000	-0.0903	0.0024	0.0032	0.3721	0.2875
23000	-0.0917	0.0024	0.0033	0.3658	0.2798
24000	-0.0931	0.0024	0.0035	0.3600	0.2728
25000	-0.0944	0.0024	0.0036	0.3548	0.2664
26000	-0.0957	0.0024	0.0038	0.3500	0.2605
27000	-0.0969	0.0023	0.0039	0.3457	0.2551
28000	-0.0981	0.0023	0.0040	0.3417	0.2500
29000	-0.0993	0.0023	0.0042	0.3381	0.2453
30000	-0.1004	0.0022	0.0043	0.3347	0.2409
31000	-0.1014	0.0022	0.0044	0.3315	0.2368
32000	-0.1025	0.0022	0.0046	0.3286	0.2329
33000	-0.1035	0.0021	0.0047	0.3259	0.2293
34000	-0.1045	0.0021	0.0048	0.3234	0.2259
35000	-0.1055	0.0021	0.0050	0.3210	0.2227
36000	-0.1064	0.0020	0.0051	0.3188	0.2196
37000	-0.1073	0.0020	0.0053	0.3167	0.2167
38000	-0.1082	0.0020	0.0054	0.3147	0.2140
39000	-0.1090	0.0019	0.0055	0.3129	0.2114
40000	-0.1099	0.0019	0.0057	0.3111	0.2089

T, K	$\tilde{b}_{ae}^{\text{sc,singlet}}$, s-wave	$\tilde{b}_{ae}^{\text{sc,singlet}}$, p-wave	$\tilde{b}_{ae}^{\text{sc,singlet}}$, d-wave	$\tilde{b}_{ae}^{\text{bound,singlet}}$	$\tilde{b}_{ae}^{\text{singlet}}$ full
41000	-0.1107	0.0019	0.0058	0.3095	0.2065
42000	-0.1115	0.0018	0.0060	0.3079	0.2043
43000	-0.1123	0.0018	0.0061	0.3064	0.2021
44000	-0.1130	0.0018	0.0063	0.3050	0.2001
45000	-0.1138	0.0018	0.0064	0.3036	0.1981
46000	-0.1145	0.0017	0.0066	0.3024	0.1962
47000	-0.1152	0.0017	0.0067	0.3011	0.1944
48000	-0.1159	0.0017	0.0069	0.3000	0.1927
49000	-0.1166	0.0017	0.0070	0.2989	0.1910
50000	-0.1172	0.0016	0.0072	0.2978	0.1894
51000	-0.1179	0.0016	0.0073	0.2968	0.1879
52000	-0.1185	0.0016	0.0075	0.2958	0.1864
53000	-0.1191	0.0016	0.0076	0.2949	0.1850
54000	-0.1197	0.0015	0.0078	0.2940	0.1837
55000	-0.1203	0.0015	0.0079	0.2931	0.1823
56000	-0.1208	0.0015	0.0081	0.2923	0.1811
57000	-0.1214	0.0015	0.0083	0.2915	0.1799
58000	-0.1219	0.0015	0.0084	0.2907	0.1787
59000	-0.1225	0.0015	0.0086	0.2899	0.1776
60000	-0.1230	0.0015	0.0088	0.2892	0.1765
61000	-0.1235	0.0015	0.0089	0.2885	0.1755
62000	-0.1240	0.0015	0.0091	0.2879	0.1745
63000	-0.1245	0.0015	0.0093	0.2872	0.1735
64000	-0.1250	0.0015	0.0095	0.2866	0.1726
65000	-0.1254	0.0015	0.0096	0.2860	0.1717
66000	-0.1259	0.0015	0.0098	0.2854	0.1709
67000	-0.1263	0.0015	0.0100	0.2848	0.1700
68000	-0.1268	0.0015	0.0102	0.2843	0.1693
69000	-0.1272	0.0015	0.0104	0.2838	0.1685
70000	-0.1276	0.0015	0.0105	0.2833	0.1678
71000	-0.1280	0.0015	0.0107	0.2828	0.1671
72000	-0.1284	0.0015	0.0109	0.2823	0.1664
73000	-0.1288	0.0015	0.0111	0.2818	0.1658
74000	-0.1291	0.0016	0.0113	0.2813	0.1651
75000	-0.1295	0.0016	0.0115	0.2809	0.1645
76000	-0.1299	0.0016	0.0117	0.2805	0.1640
77000	-0.1302	0.0016	0.0119	0.2801	0.1634
78000	-0.1306	0.0017	0.0121	0.2796	0.1629
79000	-0.1309	0.0017	0.0123	0.2793	0.1624

T, K	$\tilde{b}_{ae}^{\text{sc,singlet}}$, s-wave	$\tilde{b}_{ae}^{\text{sc,singlet}}$, p-wave	$\tilde{b}_{ae}^{\text{sc,singlet}}$, d-wave	$\tilde{b}_{ae}^{\text{bound,singlet}}$	$\tilde{b}_{ae}^{\text{singlet}}$ full
80000	-0.1312	0.0017	0.0125	0.2789	0.1620
81000	-0.1315	0.0018	0.0128	0.2785	0.1615
82000	-0.1318	0.0018	0.0130	0.2781	0.1611
83000	-0.1321	0.0018	0.0132	0.2778	0.1607
84000	-0.1324	0.0019	0.0134	0.2774	0.1603
85000	-0.1327	0.0019	0.0136	0.2771	0.1599
86000	-0.1330	0.0020	0.0139	0.2767	0.1596
87000	-0.1333	0.0020	0.0141	0.2764	0.1593
88000	-0.1335	0.0020	0.0143	0.2761	0.1590
89000	-0.1338	0.0021	0.0145	0.2758	0.1587
90000	-0.1340	0.0022	0.0148	0.2755	0.1584
91000	-0.1343	0.0022	0.0150	0.2752	0.1582
92000	-0.1345	0.0023	0.0152	0.2749	0.1580
93000	-0.1347	0.0023	0.0155	0.2746	0.1578
94000	-0.1349	0.0024	0.0157	0.2744	0.1576
95000	-0.1352	0.0025	0.0160	0.2741	0.1574
96000	-0.1354	0.0025	0.0162	0.2738	0.1573
97000	-0.1356	0.0026	0.0165	0.2736	0.1571
98000	-0.1358	0.0027	0.0167	0.2733	0.1570
99000	-0.1359	0.0027	0.0170	0.2731	0.1569
100000	-0.1361	0.0028	0.0172	0.2728	0.1568

Table 6.2: The triplet scattering part of the second virial coefficient for $e - H$ interaction. Contribution of different partial waves, last coloumn: full second virial coefficient $\tilde{b}_{ae}$.

T, K	$\tilde{b}_{ae}^{\mathrm{sc,triplet}}$, s-wave	$\tilde{b}_{ae}^{\mathrm{sc,triplet}}$, p-wave	$\tilde{b}_{ae}^{\mathrm{sc,triplet}}$, d-wave	$\tilde{b}_{ae}^{\mathrm{triplet}}$ full	$\tilde{b}_{ae}$ full
5000	-0.0548	0.0121	0.0024	-0.0402	1.3519
6000	-0.0604	0.0147	0.0029	-0.0426	0.9812
7000	-0.0654	0.0174	0.0033	-0.0446	0.7735
8000	-0.0702	0.0200	0.0038	-0.0462	0.6425
9000	-0.0746	0.0227	0.0043	-0.0475	0.5529
10000	-0.0788	0.0254	0.0048	-0.0485	0.4880
11000	-0.0828	0.0281	0.0053	-0.0494	0.4389
12000	-0.0866	0.0307	0.0057	-0.0501	0.4004
13000	-0.0902	0.0333	0.0062	-0.0506	0.3695
14000	-0.0937	0.0360	0.0067	-0.0510	0.3442
15000	-0.0970	0.0386	0.0071	-0.0512	0.3230
16000	-0.1002	0.0411	0.0076	-0.0514	0.3050
17000	-0.1034	0.0437	0.0080	-0.0515	0.2895
18000	-0.1064	0.0462	0.0085	-0.0515	0.2761
19000	-0.1093	0.0487	0.0090	-0.0515	0.2643
20000	-0.1121	0.0512	0.0094	-0.0514	0.2539
21000	-0.1149	0.0536	0.0099	-0.0513	0.2447
22000	-0.1176	0.0560	0.0103	-0.0511	0.2364
23000	-0.1202	0.0584	0.0108	-0.0508	0.2289
24000	-0.1227	0.0608	0.0112	-0.0506	0.2222
25000	-0.1252	0.0631	0.0117	-0.0503	0.2161
26000	-0.1276	0.0654	0.0121	-0.0500	0.2105
27000	-0.1300	0.0676	0.0126	-0.0496	0.2054
28000	-0.1323	0.0699	0.0130	-0.0493	0.2007
29000	-0.1345	0.0721	0.0135	-0.0489	0.1964
30000	-0.1367	0.0742	0.0139	-0.0485	0.1924
31000	-0.1389	0.0764	0.0144	-0.0481	0.1887
32000	-0.1410	0.0785	0.0148	-0.0477	0.1852
33000	-0.1431	0.0806	0.0152	-0.0472	0.1820
34000	-0.1452	0.0826	0.0157	-0.0468	0.1791
35000	-0.1472	0.0846	0.0161	-0.0463	0.1763
36000	-0.1491	0.0866	0.0165	-0.0459	0.1737
37000	-0.1511	0.0886	0.0170	-0.0454	0.1712
38000	-0.1530	0.0905	0.0174	-0.0450	0.1690
39000	-0.1548	0.0924	0.0178	-0.0445	0.1668
40000	-0.1567	0.0943	0.0183	-0.0440	0.1648

T, K	$\tilde{b}_{ae}^{\text{sc,triplet}}$, s-wave	$\tilde{b}_{ae}^{\text{sc,triplet}}$, p-wave	$\tilde{b}_{ae}^{\text{sc,triplet}}$, d-wave	$\tilde{b}_{ae}^{\text{triplet}}$ full	$\tilde{b}_{ae}$ full
41000	-0.1585	0.0962	0.0187	-0.0435	0.1629
42000	-0.1603	0.0980	0.0191	-0.0431	0.1611
43000	-0.1620	0.0998	0.0195	-0.0426	0.1595
44000	-0.1637	0.1016	0.0199	-0.0421	0.1579
45000	-0.1654	0.1033	0.0204	-0.0417	0.1564
46000	-0.1671	0.1050	0.0208	-0.0412	0.1550
47000	-0.1687	0.1067	0.0212	-0.0407	0.1536
48000	-0.1704	0.1084	0.0216	-0.0402	0.1524
49000	-0.1720	0.1101	0.0220	-0.0398	0.1512
50000	-0.1735	0.1117	0.0224	-0.0393	0.1501
51000	-0.1751	0.1133	0.0228	-0.0388	0.1490
52000	-0.1766	0.1149	0.0232	-0.0384	0.1480
53000	-0.1782	0.1165	0.0236	-0.0379	0.1471
54000	-0.1796	0.1181	0.0240	-0.0374	0.1462
55000	-0.1811	0.1196	0.0244	-0.0370	0.1453
56000	-0.1826	0.1211	0.0248	-0.0365	0.1445
57000	-0.1840	0.1226	0.0252	-0.0361	0.1438
58000	-0.1854	0.1241	0.0256	-0.0356	0.1431
59000	-0.1868	0.1255	0.0260	-0.0352	0.1424
60000	-0.1882	0.1270	0.0264	-0.0347	0.1418
61000	-0.1896	0.1284	0.0268	-0.0343	0.1412
62000	-0.1909	0.1298	0.0272	-0.0338	0.1406
63000	-0.1923	0.1312	0.0276	-0.0334	0.1401
64000	-0.1936	0.1326	0.0280	-0.0330	0.1396
65000	-0.1949	0.1339	0.0283	-0.0325	0.1391
66000	-0.1962	0.1353	0.0287	-0.0321	0.1387
67000	-0.1974	0.1366	0.0291	-0.0317	0.1383
68000	-0.1987	0.1379	0.0295	-0.0313	0.1379
69000	-0.2000	0.1392	0.0298	-0.0308	0.1376
70000	-0.2012	0.1405	0.0302	-0.0304	0.1373
71000	-0.2024	0.1417	0.0306	-0.0300	0.1370
72000	-0.2036	0.1430	0.0309	-0.0296	0.1368
73000	-0.2048	0.1442	0.0313	-0.0292	0.1365
74000	-0.2060	0.1454	0.0317	-0.0288	0.1363
75000	-0.2071	0.1467	0.0320	-0.0284	0.1361
76000	-0.2083	0.1479	0.0324	-0.0280	0.1360
77000	-0.2094	0.1490	0.0327	-0.0276	0.1358
78000	-0.2106	0.1502	0.0331	-0.0272	0.1357
79000	-0.2117	0.1514	0.0334	-0.0268	0.1356

T, K	$\tilde{b}_{ae}^{\text{sc,triplet}}$, s-wave	$\tilde{b}_{ae}^{\text{sc,triplet}}$, p-wave	$\tilde{b}_{ae}^{\text{sc,triplet}}$, d-wave	$\tilde{b}_{ae}^{\text{triplet}}$ full	$\tilde{b}_{ae}$ full
80000	-0.2128	0.1525	0.0338	-0.0264	0.1355
81000	-0.2139	0.1537	0.0341	-0.0260	0.1355
82000	-0.2150	0.1548	0.0345	-0.0256	0.1354
83000	-0.2161	0.1559	0.0348	-0.0252	0.1354
84000	-0.2171	0.1570	0.0352	-0.0248	0.1354
85000	-0.2182	0.1581	0.0355	-0.0244	0.1355
86000	-0.2192	0.1592	0.0358	-0.0241	0.1355
87000	-0.2202	0.1603	0.0362	-0.0237	0.1356
88000	-0.2213	0.1614	0.0365	-0.0233	0.1356
89000	-0.2223	0.1624	0.0368	-0.0229	0.1357
90000	-0.2233	0.1635	0.0372	-0.0226	0.1358
91000	-0.2243	0.1645	0.0375	-0.0222	0.1360
92000	-0.2253	0.1655	0.0378	-0.0218	0.1361
93000	-0.2262	0.1666	0.0381	-0.0214	0.1363
94000	-0.2272	0.1676	0.0385	-0.0211	0.1365
95000	-0.2282	0.1686	0.0388	-0.0207	0.1367
96000	-0.2291	0.1696	0.0391	-0.0203	0.1369
97000	-0.2300	0.1706	0.0394	-0.0200	0.1371
98000	-0.2310	0.1716	0.0397	-0.0196	0.1374
99000	-0.2319	0.1725	0.0400	-0.0192	0.1376
100000	-0.2328	0.1735	0.0403	-0.0189	0.1379

6.4   Generalized Beth-Uhlenbeck approach

The virial expansion can be extended to higher densities if the effects of the medium are taken into account. In particular, we outline the consequence of Pauli blocking on the two-particle properties, that is of importance when the electrons become degenerate. There are other medium effects such as screening, where the effective interaction potential between the electron and the atom is replaced by a screened potential. The influence on the scattering processes using screened versions of the Buckingham and the RDO models has been treated in Refs. [Red97, RDO05] and will not repeated here. A systematic approach to screening effects is given within the Green's function theory [WDWG86].

We consider the two-particle effective wave equation

$$
\left[\frac{p_1^2}{2m_1} + \Delta^{\mathrm{SE}}(p_1) + \frac{p_2^2}{2m_2} + \Delta^{\mathrm{SE}}(p_2) \right] \psi(p_1, p_2) +
$$
$$
\left[1 \pm f(p_1) \pm f(p_2) \right] \sum_{p_1', p_2'} V(p_1 p_2, p_1' p_2') \psi(p_1', p_2')
$$
$$
= E(P, T, \mu_c) \psi(p_1, p_2) , \qquad (6.11)
$$

where $\Delta^{\mathrm{SE}}(p)$ denotes the self-energy shift, and $f(p) = 1/\left(\exp\left[\beta(\frac{p^2}{2m} - \mu) \right] \mp 1 \right)$ are the Bose and Fermi distributions. This approach has been applied to charged-particle systems as detailed in Ref. [WDWG86] for the electron-ion system as well as for the electron-hole system. We will use a similar approach for the $e - a$ problem.

The inclusion of self-energy, screening and Pauli blocking effects in the solution of the in-medium Schrödinger equation for the electron-ion system leads to non-ideality contributions. In particular, the Mott effect is obtained, i.e. the dissolution of bound states in the continuum of scattering states at increased densities. The contribution of the energy shift of atomic levels on the thermodynamics of the dense hydrogen was considered in Refs [WWD76, WDWG86]. The Pauli shift $\Delta^{\mathrm{Pauli}} = 32\pi n_e$ (in Rydberg units) at low temperatures and at low densities and the Fock shift $\Delta^{\mathrm{Fock}} = -20\pi n_e$, lead to modified behavior at high pressures. In Ref. [SJR89], the effects of Pauli blocking on transport properties of dense plasma were investigated by solving the thermodynamical T-matrix for the electron-ion scattering for a separable electron-ion potential.

A generalized Beth-Uhlenbeck formula has been successfully elaborated for nuclear matter [SRS90]. In particular, the Mott effect can be included so that the applicability of this approach is extended to the region where a quasiparticle description is possible, e.g. in the region of strong degeneracy. Analytical expressions are derived for a separable potential approach where the in-medium T-matrix including Pauli blocking effects can be calculated.

We study the shift of the binding energy of H$^-$ as well as the modification of $e - a$ scattering phase-shifts due to Pauli blocking. Our starting point is the effective Schrödinger

equation for the $e - a$ problem

$$\left[\frac{p^2}{2m} + \Delta^{\mathrm{SE}}(p)\right]\psi(p) + \left[1 - f(p)\right]\sum_{p'} V(p, p')\psi(p') = E_0\psi(p).$$ (6.12)

Medium effects are the self-energy (Fock term) $\Delta^{\mathrm{SE}}(p)$ and the Pauli blocking term $[1 - f(p)]$, that describes the occupation of phase space.

To investigate the Mott effect with respect to the formation of H^-, we investigate the binding energy of the $e - a$ system as a function of density, i.e. the difference between the bound state energy and the continuum edge of scattering states. The self-energy of electrons $\Delta^{\mathrm{SE}}(p)$ due to the electron-atom interaction shifts both the bound state energy as well as the scattering states, the net effect on the ionization energy hence being zero. The leading term is the Pauli blocking term, that will be evaluated in the following.

We determine the occupation number $f(p)$ in Eq.(6.12) via the chemical potential μ_e according to

$$\int_0^\infty \frac{d^3p}{(2\pi\hbar)^3} \frac{1}{\exp\left[\beta(\frac{p^2}{2m_e} - \mu_e)\right] + 1} = \frac{n_e}{2}.$$ (6.13)
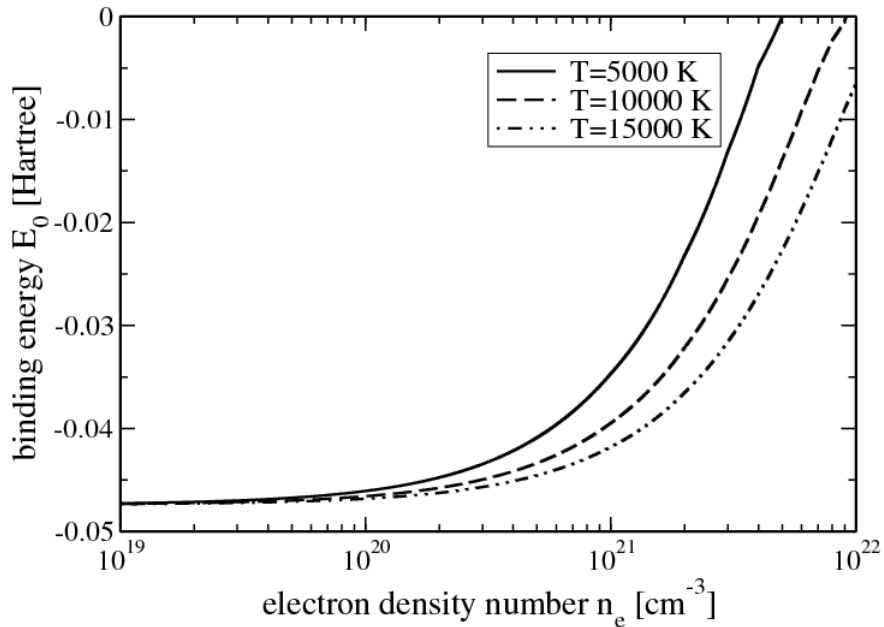

Figure 6.9: H^- binding energy in dependence of total electron number density n_e for different temperatures T.
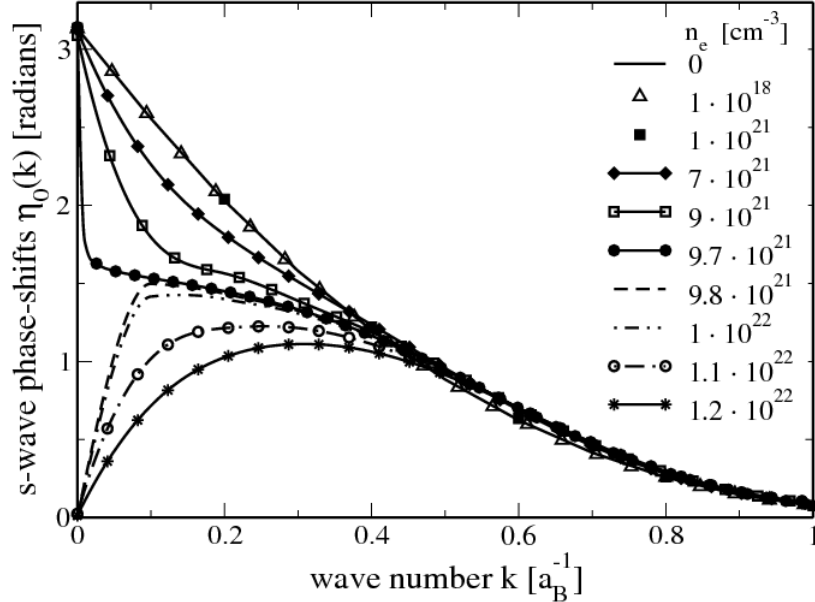
Figure 6.10: s-wave scattering phase-shifts as function of wavenumber k for different electron densities n_e at $T = 10000$ K. For comparison, the low-density limit ($n_e = 0$) is also shown.

Using the parameters of the rank-one separable potential given in Tab. I, the binding energies of the electron in the negative hydrogen ion have been calculated in dependence of the total electron density and the temperature. The numerical results for the in-medium binding energies are given in Fig. 6.9. We see that the binding energy is decreased with increasing electron density. For $T = 10000$ K, at the density exceeding the Mott density $n_e^{\mathrm{Mott}} = 9.8 \cdot 10^{21}$ cm^{-3}, bound states cannot be formed.

The influence of the medium on the scattering phase-shifts is obtained by solving the T-matrix including the Pauli blocking term. Results for different densities are presented in Fig. 6.10. At the Mott density we observe a jump of the in-medium s-wave phase-shift η_0 by π according to the Levinson theorem.

Using the density dependent phase-shifts and binding energies calculated from the in-medium Schrödinger equation (6.12), we can calculate the scattering and bound parts of the second virial coefficient.

The results are summarized in Tabs. 6.3 and 6.4. With increasing density the bound part of the second virial coefficient is decreasing because the binding energy becomes smaller due to the Pauli blocking and screening effects.

It should be mentioned that the account of the self-energy $\Delta^{\mathrm{SE}}(p)$ would contribute to the chemical potential as determined by the normalization condition (6.13). If the density of the electrons is replaced by the density of quasiparticles that account for the self-energy

Table 6.3: Results only for s -wave:the singlet scattering part of the second virial coefficient $\tilde{b}_{ae}^{\mathrm{sc,singlet}}(T, n_e)$ for $e - H$ interaction for different electron number densities and temperatures. The phase-shifts are calculated with the separable model.

T, K	$n_e = 10^{18}\mathrm{cm}^{-3}$	$n_e = 10^{19}\mathrm{cm}^{-3}$	$n_e = 10^{21}\mathrm{cm}^{-3}$	$n_e = 5*10^{21}\mathrm{cm}^{-3}$
5000	-0.0505	-0.0504	-0.0464	-0.1012
6000	-0.0547	-0.0546	-0.0521	-0.0764
7000	-0.0584	-0.0583	-0.0571	-0.0750
8000	-0.0617	-0.0616	-0.0614	-0.0770
9000	-0.0647	-0.0646	-0.0653	-0.0797
10000	-0.0674	-0.0674	-0.0688	-0.0825
11000	-0.0700	-0.0700	-0.0708	-0.0851
12000	-0.0725	-0.0725	-0.0729	-0.0871
13000	-0.0748	-0.0748	-0.0755	-0.0894
14000	-0.0770	-0.0770	-0.0772	-0.0917
15000	-0.0792	-0.0792	-0.0794	-0.0939

shift, we also have to modify the Beth-Uhlenbeck expression for the second virial coefficient as shown in Ref. [SRS90]. The Beth-Uhlenbeck expression for the second virial coefficient (5.20) used here is consistent with the single particle contribution given by free particles as done here. In future investigations, an improved treatment of density effect can be performed on the basis of quasiparticles and their corresponding screened interactions.

Table 6.4: The bound part of the second virial coefficient $\tilde{b}_{ae}^{\text{bound,singlet}}(T, n_e)$ for $e - H$ interaction for different electron number densities.

T, K	$n_e = 10^{17}\text{cm}^{-3}$	$n_e = 10^{19}\text{cm}^{-3}$	$n_e = 10^{21}\text{cm}^{-3}$	$n_e = 5 * 10^{21}\text{cm}^{-3}$
5000	4.8698	4.8298	2.1955	0.2505
6000	2.9688	2.9506	1.6384	0.2865
7000	2.0848	2.0749	1.3154	0.3243
8000	1.5993	1.5932	1.1080	0.3529
9000	1.3013	1.2973	0.9650	0.3730
10000	1.1034	1.1006	0.8610	0.3864
11000	0.9640	0.9620	0.7824	0.3948
12000	0.8615	0.8599	0.7210	0.3996
13000	0.7833	0.7820	0.6719	0.4019
14000	0.7219	0.7209	0.6318	0.4023
15000	0.6726	0.6718	0.5984	0.4015

Conclusions

For partially ionized plasmas, the cluster virial expansion for thermodynamic functions has been considered. We focus on the contribution due to the electron-atom interaction. With the help of the Beth-Uhlenbeck formula, the second virial coefficient in the electron-atom channel is related to phase-shifts and possible bound states in that channel. In contrast to former approaches, we give values for the second virial coefficient in the $e - a$ channel that are not based on any pseudopotential models but are directly related to measured data. Depending on the accuracy of presently available experimental data, these exact results for the second virial coefficient can serve as a benchmark to test other more empirical approaches using pseudopotentials or related concepts to evaluate the thermodynamic properties of partially ionized plasmas.

From the theoretical point of view, the $e - a$ interaction amounts to a three-particle problem. At present, the most reliable numerical solutions are obtained from variational calculations. After comparing these results with experimental scattering data, the second virial coefficient has been presented in the range from 5×10^3 to 10^5 K.

The accurate calculation of the free energy excess due to electron-atom interaction is compared with excluded volume results that are widely used in the chemical model. This semi-empirical treatment contains the hard-core radius of the atom as an empirical parameter. Comparing the corresponding virial expansions, it is shown that a single parameter choice for the hard-core radius cannot reproduce the nonideal contribution to the thermodynamic functions in a wide region of temperature.

We also considered different empirical pseudopotentials that can approximate these microscopic input quantities. In particular, a rank-two separable potential was introduced that fits the microscopic data. The advantage of a properly chosen pseudopotential is that higher order non-ideality terms with respect to the density can be calculated. For this, the on-shell properties in the two-body channel are no longer sufficient.

Going beyond the second virial coefficient, density effects such as self-energy shifts and Pauli blocking have to be considered. In particular, we have included Pauli blocking using the separable potential. In this way, we performed calculations for the density dependent second virial coefficient to cover a larger region with respect to the density.

Our study of the contribution of the electron-atom interaction is a step to the systematic evaluation of the thermodynamics of partially ionized dense plasma where artificial parameters such as a hard-core radius are obsolete. The main ingredient, the systematic transition from the physical picture to a chemical one, can be obtained from a quantum statistical approach. The use of the technique of Green's functions allows for the account of higher order many-particle effects. The generalization of the cluster-virial expansion, including more bound states as well as excited states, is straightforward.

Bibliography

[Arm68]   R. L. Armstead. *Phys. Rev.*, 171:91, 1968.

[AS64]   M. Abramowitz and I. A. Stegun. *Handbook of Mathematical Functions.* Dover, New York, 1964.

[Bab76]   V. V. Babikov. *The Method of Phase Functions in Quantum Mechanics.* Moscow, 1976.

[BEF99]   D. Beule, W. Ebeling, and A. Frster. *Phys. Rev. B*, 59:14177, 1999.

[BF58]   R.T. Brackmann and W.L. Fite. *Phys.Rev.*, 112:1157, 1958.

[Bha07]   A.K. Bhatia. *Phys.Rev.A*, 75:032713, 2007.

[BNRR97]   A. Bunker, S. Nagel, R. Redmer, and G. Röpke. *Phys. Rev. B*, 56:3094, 1997.

[BSW67]   P.G. Burke, S.Ormonde, and W. Whitaker. *Proc.Phys.Soc.Lond.*, 92:319, 1967.

[BU37]   E. Beth and G. E. Uhlenbeck, 1937.

[Col98]   G. W. Collins. *Science*, 281:1178, 1998.

[CP98]   G. Chabrier and A. Y. Potekhin. *Phys. Rev. E*, 58:4941, 1998.

[Deu77]   C. Deutsch. *Phys. Lett. A*, 60:317, 1977.

[DFG81]   C. Deutsch, Y. Furutani, and M.G. Gombert. *Phys.Rep.*, 69:86, 1981.

[Dra06]   R. P. Drake. *High-energy-density physics: fundamentals, inertial fusion, and experimental astrophysics.* Springer, Berlin Heidelberg, 2006.

[EFF+91]   W. Ebeling, A. Förster, V. E. Fortov, V. K. Gryaznov, and A. Ya. Polishchuk. *Thermophysical Properties of Hot Dense Plasmas.* Teubner, Stutgart, 1991.

[Eis69]   P.N. Eisner. PhD thesis, New York, 1969.

[EKK77]   W. Ebeling, W. D. Kraeft, and D. Kremp. *Theory of Bound States and Ionization Equilibrium in Plasmas and Solids.* Akademie-Verlag, Berlin, 1977.

[ER5b]   W. Ebeling and W. Richert. *Phys. Stat. Sol.*, 128:467, 1985b.

[EST73]   D. J. Ernst, S. M. Shakin, and R. M. Thaler. *Phys. Rev. C*, 8:46, 1973.

[F.C67]   F.Calogero. *Variable phase approach to potential scattering*. New York, 1967.

[FSW08]   H. Fehske, R. Schneider, and A. Weisse. *Computational Many-Particle Physics*, volume 739. Springer, Berlin, 2008.

[FWE$^+$07]   M. V. Faasen, A. Wasserman, E. Engel, F. Zhang, and K. Burke. *Phys. Rev. Lett.*, 99:043005, 2007.

[FY98]   V. E. Fortov and I. T. Yakubov. *The Physics of Non-Ideal Plasma*. World Scientific Pub Co, Singapore, 1998.

[Gel73]   S. Geltman. *J. Quant.Spectrosc.Radiat.Transfer.*, 13:601, 1973.

[GHR69]   H. C. Graboske, D. J. Harwood, and F. J. Rogers. *Phys. Rev.*, 186:210, 1969.

[GSF61]   H. B. Gilbody, R. F. Stebbings, and W. L. Fite. *Phys. Rev.*, 121:784, 1961.

[GSHS04]   T. Guillot, D. J. Stevenson, W. B. Hubbard, and D. Saumon. *Jupiter. The Planet, Satellites and Magnetosphere*. Cambridge University Press, Cambridge, 2004.

[GY52]   A.E. Glauberman and I.R. Yukhnovskiy. *JETP*, 22:562, 1952.

[HM32]   H.S.W.Massey and C.B.O. Mohr. *Proc.Roy.Soc. A*, 136:289, 1932.

[HNR07a]   B. Holst, N. Nettelmann, and R. Redmer. *Contrib. Plasma Phys.*, 47:368, 2007.

[HNR07b]   B. Holst, N. Nettelmann, and R. Redmer. *Contrib. Plas. Phys.*, 47:368, 2007.

[HS06]   C. J. Horowitz and A. Schwenk. *Nucl. Phys. A*, 776:55, 2006.

[htt]   http://nineplanets.org/.

[Hua66]   K. Huang. *Statistical Mechanics*. John Wiley and Sons, New York, 1966.

[IS92]   I.Bray and A.T. Stelbovics. *Phys.Rev.Lett.*, 69:53, 1992.

[Kel63]   G. Kelbg. *Ann. Phys.*, 12:219, 1963.

[KKK75]   W. D. Kraeft, K. Kilimann, and D. Kremp. *phys. stat. sol.(b)*, 72:461, 1975.

[KR00]   S. Kuhlbrodt and R. Redmer. *Phys. Rev. E*, 62:7191, 2000.

[KRT01]   M. Knaup, P.-G. Reinhard, and C. Toepffer. *Contrib. Plasma Phys.*, 41:159, 2001.

[KRTZ02]   M. Knaup, P.-G. Reinhard, C. Toepffer, and G. Zwicknagel. *Comput. Phys. Comm.*, 147:202, 2002.

[KSK05]   D. Kremp, M. Schlanges, and W. D. Kraeft. *Quantum Statistics of Nonideal Plasmas.* Springer, Berlin, 2005.

[LAB⁺04]   J. D. Lindl, P. Amendt, R. L. Berger, et al. *Phys. Plasmas*, 11:399, 2004.

[Lev49]   N. Levinson. *Kgl. Danske Videnskab Selskab, Mat.-fys. Medd.*, 25:1, 1949.

[Lew04]   J. S. Lewis. *Physics and chemistry of the solar system.* Elsevier Academic Press, San Diego, 2004.

[LHR09]   W. Lorenzen, B. Holst, and R. Redmer. *Phys. Rev. Lett.*, 102:115701, 2009.

[LJR08]   L.Liu, J.G.Wang, and R.K.Janev. *Phys.Rev.A*, 77:032709, 2008.

[LL88]   L.D. Landau and Y. I. Lifshits. *Quantum Mechanics*, volume 3. Moscow, 1988.

[LS50]   B. A. Lippmann and J. Schwinger. *Phys. Rev.*, 79:469, 1950.

[M.A83]   M.A.Morrison. *Aust.J.Phys*, 36:239, 1983.

[MC01]   B. Militzer and D.M. Ceperley. *Phys.Rev.E*, 63:066404, 2001.

[MF06]   V. B. Mintsev and V. E. Fortov. *J. Phys. A: Math. Gen.*, 39:4319, 2006.

[Mon69]   T. Mongan. *Phys. Rev.*, 178:1597, 1969.

[MW74]   K. E. McCulloh and J. A. Walker. *Chem. Phys. Lett.*, 25:439, 1974.

[MWE⁺07]   M.V.Faasen, A. Wasserman, E.Engel, F.Zhang, and K.Burke. *Phys.Rev.Lett.*, 99:043005, 2007.

[NMRT61]   R. Neynaber, L.L. Marino, E.W. Rothe, and S.M. Trujillo. *Phys.Rev.*, 124:135, 1961.

[NS68]   G. E. Norman and A. N. Starostin. *High Temp.*, 394:6, 1968.

[OO60]   T. Ohmura and H. Ohmura. *Phys.Rev.*, 118:154, 1960.

[ORS61]   T. O'Malley, L. Rosenberg, and L. Spruch. *J. Math. Phys.*, 2:491, 1961.

[ORS62]   T. O'Malley, L. Rosenberg, and L. Spruch. *Phys. Rev.*, 125:1300, 1962.

[PCM87]   P.G.Burke, C.J.Noble, and M.P.Scott. *Proc.Roy.Soc.A*, 410:289, 1987.

[Pek62]   C. L. Pekeris. *Phys. Rev.*, 126:1470, 1962.

[PT66]   P.G.Burke and A.J. Taylor. *Proc.Roy.Soc.*, 88:549, 1966.

[RDG+09]   T. S. Ramazanov, K. N. Dzhumagulova, M. T. Gabdullin, A. Zh. Akbar, and R. Redmer. *J. Phys. A: Math. Theor.*, 42:214049, 2009.

[RDO05]   T.S. Ramazanov, K.N. Dzhumagulova, and Yu.A. Omarbakiyeva. *Phys.Plasmas*, 12:092702, 2005.

[RDOR07]   T. S. Ramazanov, K. N. Dzhumagulova, Y. A. Omarbakiyeva, and G. Röpke. *Contrib. Plasma Phys*, 47:267, 2007.

[Red97]   R. Redmer. *Phys. Rep.*, 282:35, 1997.

[Red05]   R. Redmer. *Plasma Physics. Confinement, Transport and Collective Effects.* Springer, Berlin Heidelberg, 2005.

[RGD+03]   T. S. Ramazanov, K. Zh. Galiyev, K. N. Dzhumagulova, G. Röpke, and R. Redmer. *J. Phys. A: Math. Gen.*, 36:6173, 2003.

[RHH10]   R. Redmer, B. Holst, and F. Hensel. *Metal-to-Nonmetal Transitions.* Springer, Heidelberg Dordrecht London New York, 2010.

[RHJ+06a] R. Redmer, B. Holst, H. Juranek, N. Nettelmann, and V. Schwarz. *J. Phys. A: Math. Gen.*, 39:4479, 2006.

[RHJ+06b] R. Redmer, B. Holst, H. Juranek, N. Nettelmann, and V. Schwarz. *J. Phys. A: Math. Gen.*, 39:4479, 2006.

[Rob]   P. M. L. Robitaille. *arXiv:astro-ph/0410075v2.*

[Rog84]   F. J. Rogers. *Phys. Rev. A*, 29:868, 1984.

[Ros98]   M. Ross. *Phys. Rev. B*, 58:669, 1998.

[RP75]   D. Register and R. T. Poe. *Phys. Lett.*, 51A:431, 1975.

[RS96a]   L. Rosenberg and L. Spruch. *Phys. Rev. A*, 54:4978, 1996.

[RS96b]   L. Rosenberg and L. Spruch. *Phys. Rev. A*, 54:4985, 1996.

[RSM82]   G. Röpke, H. Schulz, and L. Münchow. *Nucl. Phys. A*, 379:536, 1982.

[RSO60]   L. Rosenberg, L. Spruch, and T. O'Malley. *Phys. Rev.*, 119:164, 1960.

[SC92]   D. Saumon and G. Chabrier. *Phys. Rev. A*, 46:2084, 1992.

[SCCea97] L.B. Da Silva, P. Celliers, G.W. Collins, and et al. *Phys. Rev. Lett.*, 78:483, 1997.

[Sch61]   C. Schwartz. *Phys. Rev.*, 124:1468, 1961.

[Sch05]   U. Schumacher. *Plasma Physics. Confinement, Transport and Collective Effects.* Springer, Berlin Heidelberg, 2005.

[SCWX00]   D. Saumon, G. Chabrier, D. J. Wagner, and X. Xie. *High Pressure Research*, 16:331, 2000.

[SJR89]   M. Schmidt, Th. Janke, and R. Redmer. *Contrib. Plasma Phys.*, 29:431, 1989.

[SJR05]   V. Schwarz, H. Juranek, and R. Redmer. *Phys. Chem. Chem. Phys.*, 7:1990, 2005.

[SK62]   M. Schlanges and D. Kremp. *Ann. Phys.*, 39:69, 1962.

[SK82]   M. Schlanges and D. Kremp. *Ann. Phys.*, 39:69, 1982.

[SR10]   N. A. Starostin and V. C. Roerich. *Contrib. Plasma Phys.*, 50:88, 2010.

[SRS90]   M. Schmidt, G. Röpke, and H. Schulz. *Ann. Phys. (NY)*, 202:57, 1990.

[SSB88]   T. Scholz, P. Scott, and P. G. Burke. *J. Phys. B*, 21:L139, 1988.

[Tem62]   A. Temkin. *Phys.Rev.*, 126:130, 1962.

[TLW74]   P.J.O. Teubner, C.R. Lloyd, and E. Weigold. *Phys.Rev.A*, 9:2552, 1974.

[TRK+10]   S. Typel, G. Röpke, T. Klähn, D. Blaschke, and H. H. Wolter. *Phys. Rev. C*, 81:015803, 2010.

[VSK04a]   J. Vorberger, M. Schlanges, and W. D. Kraeft. *Phys. Rev. E*, 69:046407, 2004.

[VSK04b]   J. Vorberger, M. Schlanges, and W.D. Kraeft. *Phys.Rev.E*, 69:046407, 2004.

[WC75]   J.F. Willams and J. Callaway. *Phys.Rev.A*, 12(2), 1975.

[WC93]   Y. D. Wang and J. Callaway. *Phys. Rev. A*, 48:2058, 1993.

[WDWG86]   W.D.Kraeft, D.Kremp, W.Ebeling, and G.Roepke. *Quantum statistics of Charged Particle Systems.* Berlin, 1986.

[Wil75]   J. F. Willams. *J. Phys. B*, 8:1683, 1975.

[Wil98]   J. F. Willams. *Aust. J. Phys.*, 51:633, 1998.

[WSY07]   W.-S.Chang and Y.D.Yung. *Physica scripta*, 76:299, 2007.

[WWD76]   W.Ebeling, W.D.Kraeft, and D.Kremp. *Theory of Bound States and Ionization Equilibrium.* Berlin, 1976.

[Yam54]   Y. Yamaguchi. *Phys. Rev*, 95:1628, 1954.

[Zim88]   R. Zimmermann. *Many-Particle Theory of Highly Excited Semiconductors.* Teubner, Leipzig, 1988.

[ZKK+78]   R. Zimmermann, K. Kilimann, W. D. Kraeft, K. Kremp, and G. Röpke. *phys. stat. sol.(b)*, 90:175, 1978.

[ZL44]   Y. B. Zeldovich and L. D. Landau. *Zh. Eksp. Teor. Fiz.*, 14:32, 1944.

Part II

Published articles

Chapter 7

The electron-atom interaction in partially ionized dense plasmas

Authors: Yultuz Omarbakiyeva, Tlekkabul Ramazanov and Gerd Röpke

Listing of contributions by authors:

- Y.O.: Preparation of the manuscript, all analytical and numerical calculations

- T.R.: Preparation of manuscript

- G.R.: Preparation of manuscript

The electron-atom interaction in partially ionized dense plasmas

Yu.A. Omarbakiyeva, T.S. Ramazanov, G.Röpke*

IETP, Al Farabi Kazakh National University,Tole Bi 96a, 050012 Almaty, Kazakhstan
* Fachberich Physik, Universität Rostock, D-18051 Rostock, Germany

E-mail: `yultuz@physics.kz`

Abstract.
    The electron-atom interaction is considered in dense partially ionized plasmas. The separable potential is constructed from scattering data using effective radius theory. Parameters of the interaction potential were obtained from phase shifts, scattering length and effective radius. The binding energy of the electron in the H^- ion is determined for the singlet channel on the basis of the reconstructed separable potential. In dense plasmas, the influence of the Pauli exclusion principle on the phase shifts and the binding energy is considered. Due to the Pauli blocking, the binding energy vanishes at the Mott density. At that density the behavior of the phase shifts are drastically changed. This leads to modifications of macroscopic properties such as composition and transport coefficients.

Chapter 8

Phase Shifts and the Second Virial Coefficient for a Partially Ionized Hydrogen Plasma

Authors: Yultuz Omarbakiyeva, Gerd Röpke and Tlekkabul Ramazanov

Listing of contributions by authors:

- Y.O.: Preparation of manuscript, all numerical calculations

- G.R.: Preparation of manuscript

- T.R.: Preparation of manuscript

Phase shifts and the second virial coefficient for a partially ionized hydrogen plasma

Y.A.Omarbakiyeva[*1,2]**, G.Röpke**[1]**,** and **T.S. Ramazanov**[2]

[1] Institut für Physik, Universität Rostock, 18051 Rostock, Germany
[2] IETP, al-Farabi Kazakh National University, 96a Tole bi str., 050012 Almaty, Kazakhstan

The influence of the interaction of electrons with hydrogen atoms on the thermodynamical properties of dense plasmas is investigated using a virial expansion approach. The second virial coefficient for the electron-atom interaction is obtained from the Beth-Uhlenbeck formula. Elastic scattering phase shifts are calculated with the help of the phase function method for different polarization potential models. Results for the second virial coefficient are given that take into account both the bound state part and the scattering state contribution.

---

* Corresponding author: e-mail:yultuz@physics.kz, Phone: 007 7272 927075, Fax: 007 7272 927075

Chapter 9

Cluster virial expansion for the equation of state of partially ionized hydrogen plasma

Authors: Yultuz Omarbakiyeva, Carsten Fortmann, Tlekkabul Ramazanov and Gerd Röpke

Listing of contributions by authors:

- Y.O.: Preparation of manuscript (mainly sections 2-5), all numerical calculations

- C.F.: Preparation of manuscript (mainly sections 1-3,6)

- T.R.: Preparation of manuscript

- G.R.: Preparation of manuscript (sections 1,6)

Cluster virial expansion for the equation of state of partially ionized hydrogen plasma

Y. A. Omarbakiyeva,[1,2,*] C. Fortmann,[3] T. S. Ramazanov,[2] and G. Röpke[1]

[1]*Institute of Physics, University of Rostock, D-18051, Rostock, Germany*
[2]*IETP, Al-Farabi Kazakh National University, 96a, Tole bi St., Almaty 050012, Kazakhstan*
[3]*Department of Physics and Astronomy, University of California Los Angeles, Los Angeles CA 90095, USA*

We study the contribution of electron-atom interaction to the equation of state for partially ionized hydrogen plasma using the cluster-virial expansion. For the first time, we use the Beth-Uhlenbeck approach to calculate the second virial coefficient for the electron-atom (bound cluster) pair from the corresponding scattering phase-shifts and binding energies. Experimental scattering cross-sections as well as phase-shifts calculated on the basis of different pseudopotential models are used as an input for the Beth-Uhlenbeck formula. By including Pauli blocking and screening in the phase-shift calculation, we generalize the cluster-virial expansion in order to cover also near solid density plasmas. We present results for the electron-atom contribution to the virial expansion and the corresponding equation of state, i.e. pressure, composition, and chemical potential as a function of density and temperature. These results are compared with semi-empirical approaches to the thermodynamics of partially ionized plasmas. Avoiding any ill-founded input quantities, the Beth-Uhlenbeck second virial coefficient for the electron-atom interaction represents a benchmark for other, semi-empirical approaches.

PACS numbers: 52.25.Kn, 52.20.Hv

*Electronic address: yultuz@physics.kz

Publication list

Publications in Peer-Review Journals

1. T. S. Ramazanov, K. N. Dzhumagulova, Y. A. Omarbakiyeva *Effective polarization interaction potential "charge-atom" for partially ionized dense plasma* Phys.Plasmas **9**, 092702 (2005).

2. T. S. Ramazanov, K. N. Dzhumagulova, Y. A. Omarbakiyeva, G. Röpke *Effective polarization interaction potentials of the partially ionized dense plasma* Journal of Physics A: Mathematical and General **39**, 4369 (2006).

3. T. S. Ramazanov, K. N. Dzhumagulova, Y. A. Omarbakiyeva, G. Roepke *Effective Polarization Potential and Scattering Processes in a Partially Ionized Plasma* Contr.Plasma Physics **47**, 267 (2007).

4. Y. A. Omarbakiyeva *Elastic scattering cross section of electrons on atoms in partially ionized plasma* (in Russian) Vestnik KazNU **23**, 55 (2007).

5. Y. A. Omarbakiyeva *Bremsstrahlung in dence semiclassical partially-ionized plasma* (in Russian) Izvestia NAN RK Physical and mathematical issue **3**, 77 (2007).

6. T. S. Ramazanov, K. N. Dzhumagulova, M. T. Gabdullin, Y. A. Omarbakiyeva *Thermodynamic and Transport Properties of Non-ideal Complex Plasma* Plasma Physics Research Advances, (2008) (accepted)

7. Y.A. Omarbakiyeva, G. Röpke, T. S. Ramazanov *The electron- atom interaction in partially ionized dense plasmas* J. Phys. A: Math. Theor. **42**, 214045 (2009)

8. Y. A. Omarbakiyeva, G. R öpke, and T. S. Ramazanov *Phase Shifts and the Second Virial Coefficient for a Partially Ionized Hydrogen Plasma* Contrib. Plasma Phys. **49**, 733 (2009)

9. Y. A. Omarbakiyeva, C. Fortmann, G. Röpke, T. S. Ramazanov, *Cluster virial expansion for the equation of state of partially ionized Hydrogen plasma* Phys.Rev. E. **82**, 026407 (2010).

Conference proceedings

1. T. S. Ramazanov, K. N. Dzhumagulova, Y. A. Omarbakiyeva *Effective polarization interaction potentials of the partially ionized plasma* Proc. XXVIIth ICPIG, 12 (2005).

2. T. S. Ramazanov, K. N. Dzhumagulova, Y. A. Omarbakiyeva, G. Röpke *Scattering processes in partially ionized plasma on the basis of the effective polarization potential* Proc. 33rd European Physical Society Conference on Plasma Physics, textbf30I, 2.054 (2006).

3. T. S. Ramazanov, K. N. Dzhumagulova, Y. A. Omarbakiyeva, G. Röpke *Electron-atom collision cross sections in partially ionized dense plasma* Proc. International conference of the plasma physics, c133p (2006).

4. T. S. Ramazanov, K. N. Dzhumagulova, Y. A. Omarbakiyeva, G. Röpke *The scattering processes in partially ionized plasma* Proc. 5 th International Conference Plasma Physics and Plasma Technology **165** 165 (2006).

5. T. S. Ramazanov, K. N. Dzhumagulova, Y. A. Omarbakiyeva, G. Röpke *Scattering of low- energy electrons by atoms of noble gas in partially ionized plasma* 34 rd EPS Conference on Plasma Phys. 2007.

6. T. S. Ramazanov, K. N. Dzhumagulova, Y. A. Omarbakiyeva, G. Röpke *Electron-atom bremsstrahlung in partially ionized plasma* 28th ICPIG 2007.

7. Y. A. Omarbakiyeva *Elastic scattering cross section of electrons on noble atoms in complex plasma* (in Russian) International congress of students, magisters and YS: World of Science 2007.

8. Y. A. Omarbakiyeva *Investigation of bremsstrahlung in partially-ionized plasma* (in Russian) 5th international scientific conference 2007.

9. Y. A. Omarbakiyeva, G. Röpke T. S. Ramazanov *The electron- atom interaction in partially ionized dense plasmas* SCCS 2008.

10. Y. A. Omarbakiyeva, G. Röpke T. S. Ramazanov *Scattering processes and the Beth-Uhlenbeck formula for a partially ionized plasma* PPPT-6 2009.

Erklärung

Ich versichere hiermit an Eides statt, dass ich die vorliegende Arbeit selbständig angefertigt und ohne fremde Hilfe verfasst habe, keine außer den von mir angegebenen Hilfsmitteln und Quellen dazu verwendet habe und die den benutzten Werken inhaltlich und wörtlich entnommenen Stellen als solche kenntlich gemacht habe.

Rostock, den

Yultuz Omarbakiyeva